Contents

List of Figures

List of Tables

Preface

This short text should serve to me, my friend or everyone interested in any topic included as a quick and useful resource of information, although originally these lines are but a summary of some problems I found interesting when studying for the state examination at the Faculty of Mathematics and Physics in the field of Particle and Nuclear Physics. Any contribution is welcomed, let it be addressing the field theory or nuclear analysis method; theory or experiment.

Miro Kladiva has contributed with the chapter on the Standard Model, which I do appreciate, just have a look at beautiful Feynman diagrams! :)

I myself am curious what this all will become and what degree may reach, initially the text was made of pieces of my diploma thesis and some more topics I was interested in.

If you have anything suitable you found nice when studying, or something from your field, don't hesitate and send me, especially I will appreciate the TEXsource file. Of course, I will properly cite authors of each part!

You are wanted!!!

Jiří Kvita
April 2003

Part I

Nuclear physics

Chapter 1

Passage of particles through matter

1.1 Photons

$\sigma_{\text{p.e.}}$ = Atomic photoelectric effect (electron ejection, photon absorption

σ_{Rayleigh} = Coherent scattering (Rayleigh scattering – atom neither ionised nor excited)

σ_{Compton} = Incoherent scattering (Compton scattering off an electron)

κ_{nuc} = Pair production in nuclear field

κ_{e} = Pair production in electron field

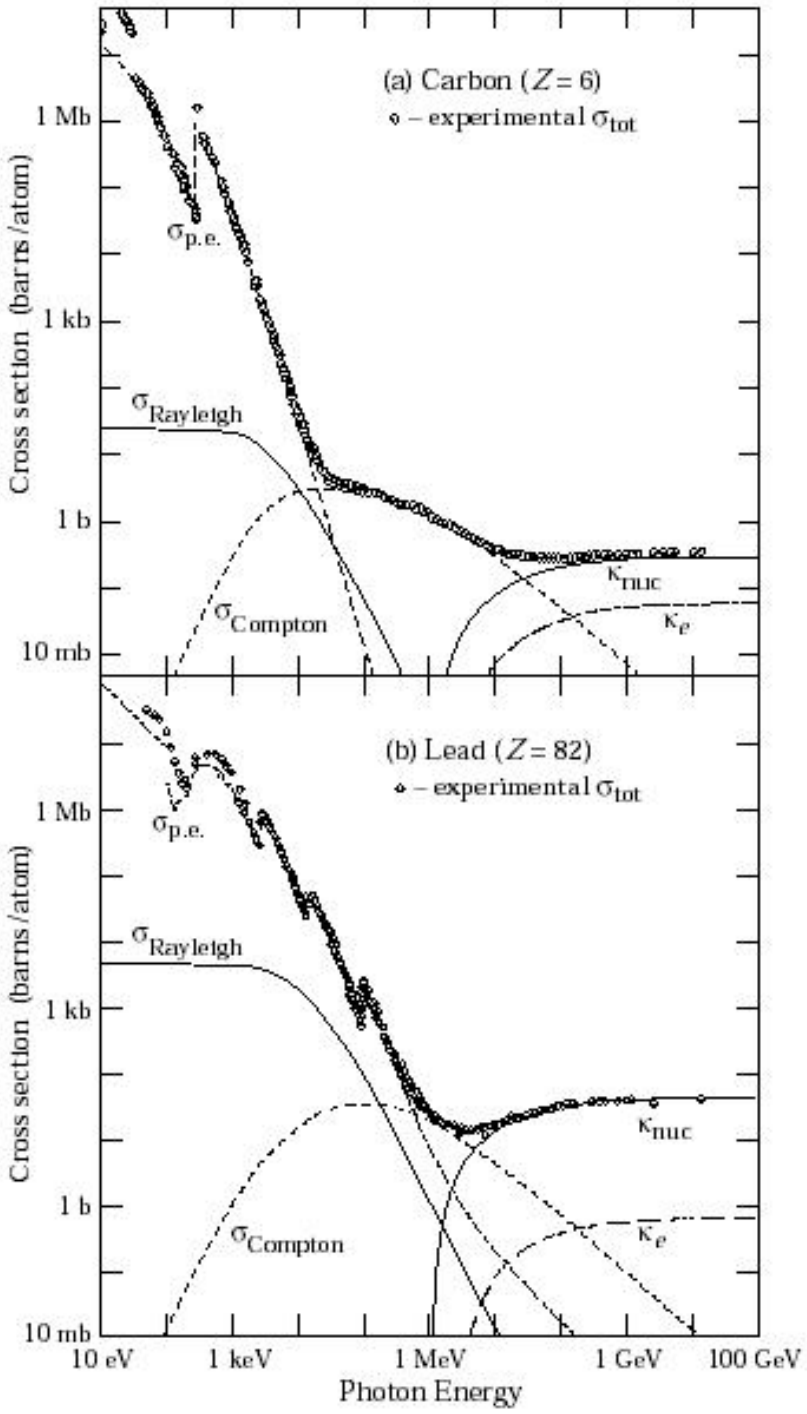

Figure 1.1: Photon total cross section as a function of energy in carbon and lead showing contributions of different processes (see in text, taken from [11])

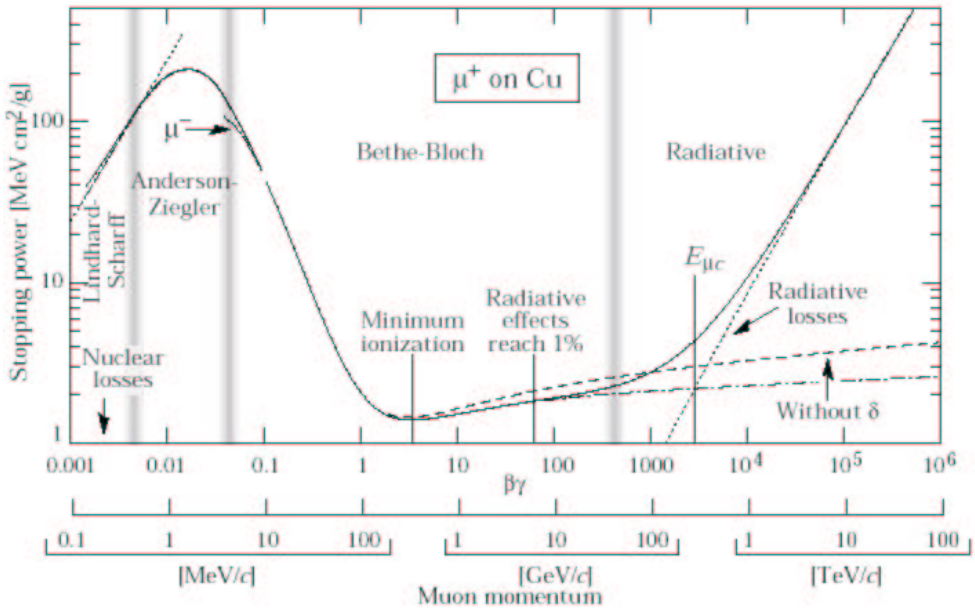

Fig. 26.1: Stopping power ($= \langle -dE/dx \rangle$) for positive muons in copper as a function of $\beta\gamma = p/Mc$ over nine orders of magnitude in momentum (12 orders of magnitude in kinetic energy). Solid curves indicate the total stopping power. Data below the break at $\beta\gamma \approx 0.1$ are taken from ICRU 49 [2], and data at higher energies are from Ref. 1. Vertical bands indicate boundaries between different approximations discussed in the text. The short dotted lines labeled "μ^-" illustrate the "Barkas effect," the dependence of stopping power on projectile charge at very low energies [6].

Figure 1.2: Stopping power for positive muons in copper (taken from [11]

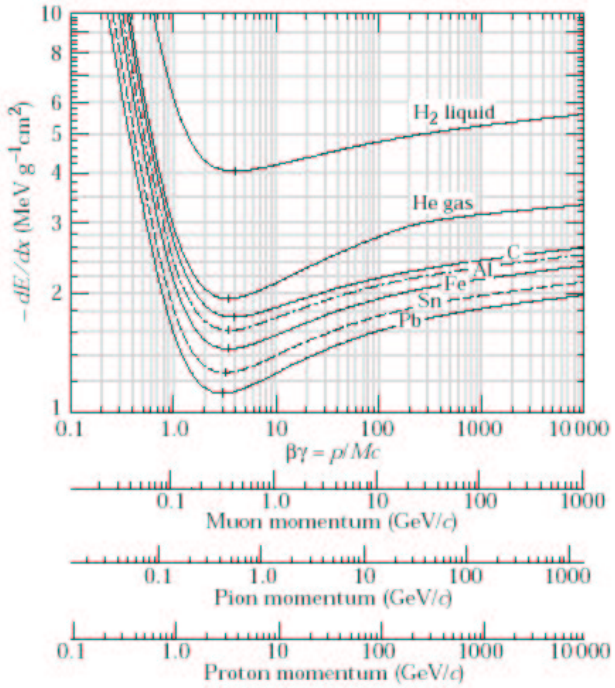

Figure 26.3: Mean energy loss rate in liquid (bubble chamber) hydrogen, gaseous helium, carbon, aluminum, iron, tin, and lead. Radiative effects, relevant for muons and pions, are not included. These become significant for muons in iron for $\beta\gamma \gtrsim 1000$, and at lower momenta for muons in higher-Z absorbers. See Fig. 26.20.

Figure 1.3: Energy losses, theoretical curves, taken from [11]

Part II

Particles and Fields

Chapter 2

Neutral pion decay – some kinematics

2.1 Basic kinematics

We study the electromagnetic decay channel of the neutral pion (branching ratio almost 100%)

$$\pi^0 \to \gamma\,\gamma$$

The fourmomenta of the two photons $P_i^* = (E_i, p_{\|}, p_{\perp})$, $i = 1, 2$ in the pion rest frame

$$P_1^* = \frac{m_\pi}{2}(1, \cos\theta^*, \sin\theta^*) \qquad P_2^* = \frac{m_\pi}{2}(1, -\cos\theta^*, -\sin\theta^*)$$

Let us study a photon with $\theta \in (0, \pi/2)$ and drop off the index 1. Then in the laboratory system, where the pion has the velocity $\vec{\beta} = (0, 0, \beta)$, the photon's fourmomentum composites will be

$$E_\gamma = \gamma(E^* + \beta p_{\|}^*) = \frac{E_\pi}{2}(1 + \beta\cos\theta^*) \tag{2.1}$$

$$p_{\|} = \gamma(p_{\|}^* + \beta E^*) = \frac{E_\pi}{2}(\cos\theta^* + \beta) \tag{2.2}$$

$$p_\perp = p_\perp^* \tag{2.3}$$

In general, all quantities in the pion rest frame are attributed with a star index *, otherwise they are assigned to the laboratory system.

2.2 Existence of the maximal angle

Measuring the scattering angle of the photon with respect to the pion's momentum one finds

$$\tan\theta = \frac{p_\perp}{p_{\|}} = \frac{p_\perp^*}{p_{\|}} = \frac{m_\pi \sin\theta^*}{E_\pi(\beta + \cos\theta^*)} = \frac{1}{\gamma}\frac{\sin\theta^*}{(\cos\theta^* + \beta)}\,. \tag{2.4}$$

Performing the derivative one can convince oneself that maximum is reached for $\theta^* = \pi/2$, and in this case we obtain the maximum scattering angle

$$\tan\theta_{\max} = \frac{m_\pi}{E_\pi} = \frac{1}{\beta\gamma}\,.$$

Outside this cone along the axis corresponding to the pion motion no forward photons can be observed!

2.3 Angular distribution of photons in the laboratory frame

Another interesting question is the angular distribution of photons in the laboratory frame. Knowing this distribution in the C.M.S.

$$\frac{\mathrm{d}N^*}{\mathrm{d}\cos\theta^*}\Big(\cos\theta^*\Big)$$

it is straightforward to come to the laboratory frame. One mustn't forget that the expression is treated as an integrand, so when changing the variable one has to include the absolute value of Jacobian. Actually, we perform a substitution

$$x = g(y)$$

$$\int f(x)\mathrm{d}x = \int f(g(y))|g'(y)|\mathrm{d}y\,.$$

where in our case

$$x = \cos\theta^*\,, \qquad y = \cos\theta\,.$$

Now we need to express $\cos\theta^*$ using $\cos\theta$.

For this purpose, (2.4) could be used, but would lead to complicated expressions. Instead, we shall make use of the inverse Lorentz transformation, which can be performed by replacing "starred" quantities with "non–starred" and vice versa, and by setting $-\beta$ instead of β/ From (2.4) we thus obtain

$$\tan\theta^* = \frac{1}{\gamma}\frac{\sin\theta^*}{(\cos\theta^* - \beta)}\,.$$

Using

$$|\cos x| = \frac{1}{\sqrt{1+\tan^2 x}}$$

and

$$\gamma^2 - 1 = \beta^2\gamma^2$$

we arrive at remarkably simple

$$\cos\theta^* = \frac{\cos\theta - \beta}{1 - \beta\cos\theta} \equiv g(\cos\theta)\,.$$

$$\Rightarrow \frac{\mathrm{d}\cos\theta^*}{\mathrm{d}\cos\theta} = \frac{1-\beta^2}{(1-\beta\cos\theta)^2} = \frac{1}{\gamma^2}\frac{1}{(1-\beta\cos\theta)^2}\,.$$

Having all we need we can now write down the result for the angular distribution in the laboratory frame

$$\frac{\mathrm{d}N}{\mathrm{d}\cos\theta} = \frac{\mathrm{d}N^*}{\mathrm{d}\cos\theta^*}\Big(g(\cos\theta)\Big)\,\frac{\mathrm{d}}{\mathrm{d}\cos\theta}\Big[g(\cos\theta)\Big] = \frac{\mathrm{d}N^*}{\mathrm{d}\cos\theta^*}\Big(g(\cos\theta)\Big)\frac{1}{\gamma^2}\frac{1}{(1-\beta\cos\theta)^2}\,.$$

Assuming a uniform distribution in C.M.S. (pion has a zero spin), the first term is but a constant and we have

$$\frac{\mathrm{d}N}{\mathrm{d}\cos\theta} = \frac{1}{4\pi}\frac{1}{\gamma^2}\frac{1}{(1-\beta\cos\theta)^2} = \frac{1}{4\pi}\frac{1-\beta^2}{(1-\beta\cos\theta)^2}\,, \qquad \theta \in (0, \theta_{\max})\,.$$

The distribution in the laboratory frame has a singularity in the maximal angle and becomes flat for $\gamma \to 1$ as expected, plots of this function can be found in Figures 2.2–2.4 (without the cut on region beyond the maximal angle).

2.4 Energy distribution of photons in Lab

From

$$E_\gamma = \frac{E_\pi}{2}(1 + \beta \cos\theta^*)$$

we have

$$\frac{\mathrm{d}E_\gamma}{\mathrm{d}\cos\theta^*} = \frac{1}{2}E_\pi\beta = \frac{p_\pi}{2} = \frac{\beta\gamma m_\pi}{2} = \frac{m_\pi}{2}\sqrt{\gamma^2 - 1}$$

As the $\cos\theta^*$ is uniformly distributed, the energy of photons in the laboratory frame is also uniformly distributed on interval depending on pion's velocity β:

$$E_\gamma^{\min} = \frac{E_\pi}{2}(1 - \beta) \qquad E_\gamma^{\max} = \frac{E_\pi}{2}(1 + \beta)\,.$$

Centre of this distribution is just $E_\pi/2$. Therefore, dealing with some spectrum of energies of pions, a peak in the gamma spectrum could be observable supporting the existence of a a neutral pion. This is exactly the way how it was discovered.

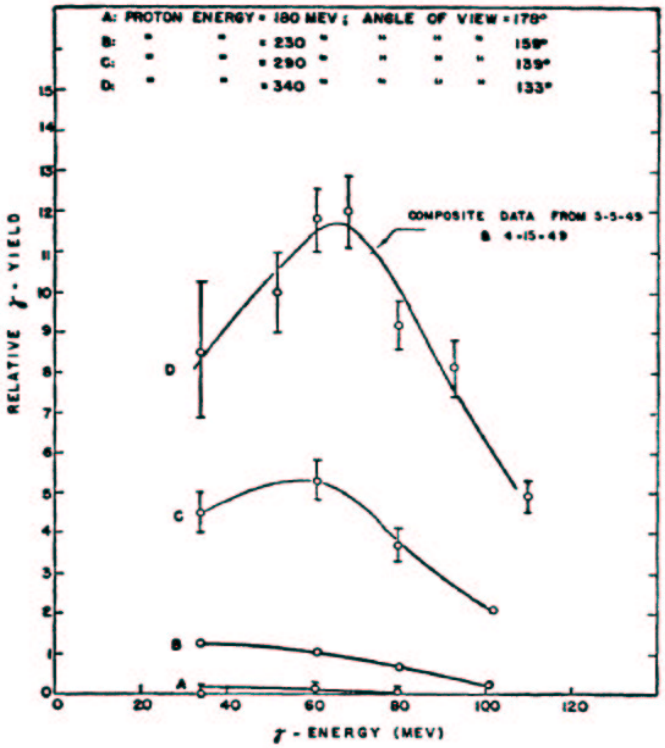

FIG. 4a. Relative gamma-yield from ½-in. carbon target at various proton energies.

Figure 2.1: Spectrum of photons from the reaction $p + C^{12}_6$ depending on proton's energy, note enhancement over the threshold for π^0 production; taken from Bjorklund R. et al., Phys. Rev. **77**, 213

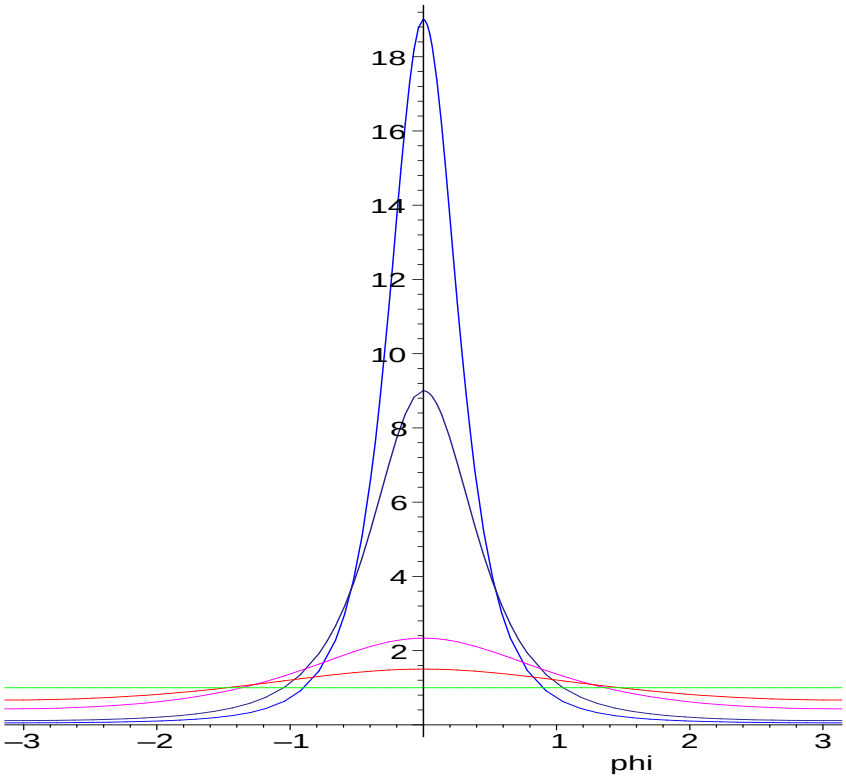

Figure 2.2: Angular distribution for photons in the laboratory frame as a function of θ, β_π =0., 0.2, 0.4, 0.8, 0.9

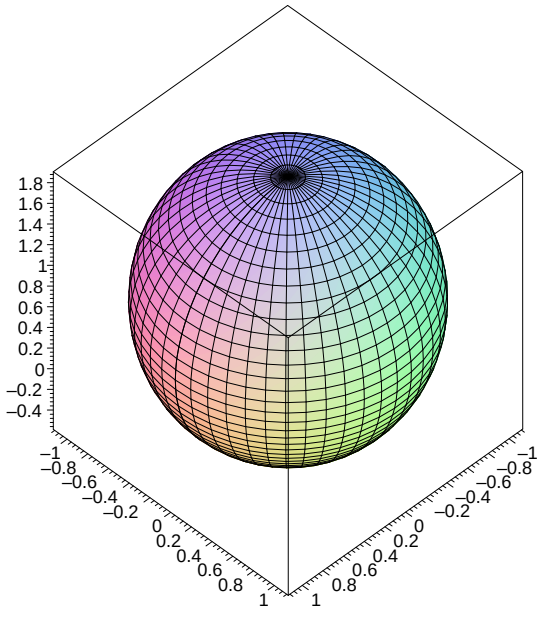

Figure 2.3: Angular distribution for photons in the laboratory frame, $\beta_\pi = 0.3$

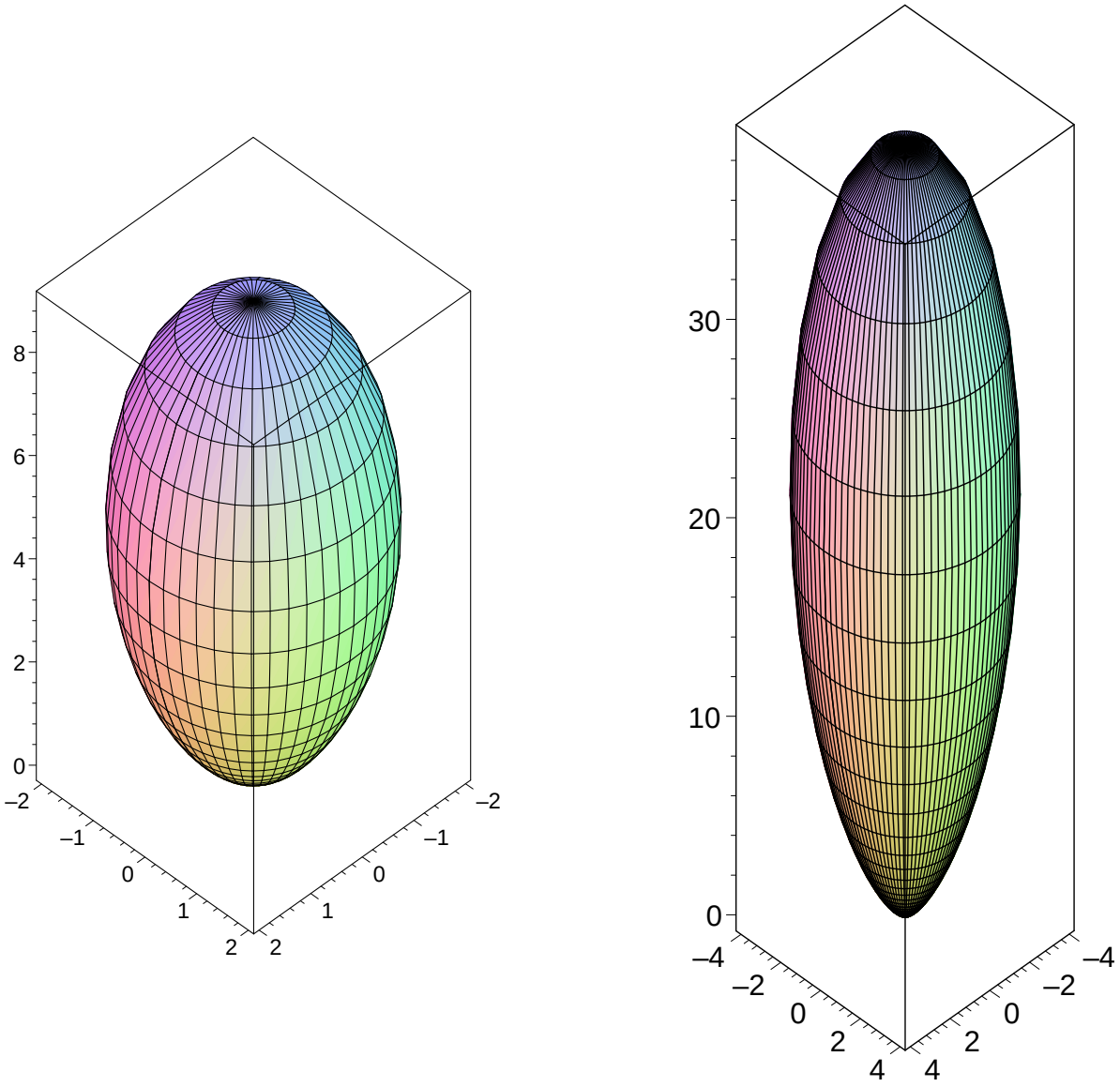

Figure 2.4: Angular distribution for photons in the laboratory frame, $\beta_\pi = 0.8, 0.95$

Chapter 3

Charged pion decay

Pion decay into leptons

$$\pi^- \to \mu^- + \bar{\nu}_\mu$$

$$\pi^- \to e^- + \bar{\nu}_e$$

expresses the ratio of corresponding decay rates (experimental value)

$$\frac{\Gamma(\pi \to e\,\nu_e)}{\Gamma(\pi \to \mu\,\nu_\mu)} = (1.230 \pm 0.004)\ \times\ 10^{-4}\,, \tag{3.1}$$

i.e. the negatively charged pion decays almost exclusively into muon and corresponding antineutrino. This may seem as a surprise, as the phase space factor appearing in Γ regardless of the model clearly prefers the electron channel (e is lighter and thus has a larger momentum in C.M.S.):

$$\frac{\mathrm{LIPS}_2(\pi \to e\,\nu_e)}{\mathrm{LIPS}_2(\pi \to \mu\,\nu_\mu)} = \frac{p_e^*}{p_\mu^*} = \frac{m_\pi^2 - m_e^2}{m_\pi^2 - m_\mu^2} \doteq 2.34\,. \tag{3.2}$$

Why, then, is the muon channel preferred by a factor of four orders of magnitude? To summarise basic features of the explanation, I used a very useful resource on Electroweak theory by J. Hořejší, ([7], pg. 69–77).

3.1 Heuristic explanation

This rather simple "explanation" is based on lectures on Elementary particle physics held by R. Leitner and finds some support in ([7], pg. 32–40, 69–77).

To start with, let us interest ourselves in the degree of polarisation of electrons emitted in a β decay process

$$n \to p\ +\ e\ +\ \bar{\nu}_e\,.$$

Defining the asymmetry in polarisations for a given energy of an electron as

$$P_e = \frac{N_\mathrm{R} - N_\mathrm{L}}{N_\mathrm{R} + N_\mathrm{L}} = \frac{\mathrm{d}w_\mathrm{R} - \mathrm{d}w_\mathrm{L}}{\mathrm{d}w_\mathrm{R} + \mathrm{d}w_\mathrm{L}}\,,$$

where N_R, N_L are numbers of electrons emitted with positive and negative helicities (positive helicity corresponding to spin oriented parallel with the electron's momentum) and $\mathrm{d}w_\mathrm{R}$, $\mathrm{d}w_\mathrm{L}$ are decay rates corresponding to positive and negative helicities.

I will not perform the whole calculation referring for details to ([7]) but only remind here that one needs to employ the formalism of describing helicity states by a spin fourvector

$$s_R(k) = \left(\frac{|\vec{k}|}{m}, \frac{E}{m} \frac{\vec{k}}{|\vec{k}|} \right) \qquad s_L(k) \equiv -s_R(k)$$

and use the projector

$$u_{e\mathrm{R}}(p)\bar{u}_{e\mathrm{R}}(p) = \frac{1}{2}(\not{p} + m_e)(1 + \gamma_5 \not{s}_{\mathrm{R}}) \,.$$

The result for a Fermi type pure V–A theory ("V minus A", vector–axial theory), i.e. a contact four fermion interaction Lagrangian where terms $\gamma^\mu(1-\gamma_5)$ appear between fermion fields, is remarkably simple:

$$P_e = -\beta_e \,,$$

proportional to electron's velocity. Therefore, for relativistic energies, almost only left handed electrons are produced.

We may now recast the result into probabilities p_e^{R}, p_e^{L} that an electron with a positive or negative helicity is emitted. Clearly

$$p_e^{\mathrm{R}} = \frac{\mathrm{d}w_{\mathrm{R}}}{\mathrm{d}w_{\mathrm{R}} + \mathrm{d}w_{\mathrm{L}}} \qquad p_e^{\mathrm{L}} = \frac{\mathrm{d}w_{\mathrm{L}}}{\mathrm{d}w_{\mathrm{R}} + \mathrm{d}w_{\mathrm{L}}} \,,$$

$$P_e = p_e^{\mathrm{R}} - p_e^{\mathrm{L}} = -\beta_e$$

and we also require

$$p_e^{\mathrm{R}} + p_e^{\mathrm{L}} = 1 \,.$$

These relations can be inverted producing

$$p_e^{\mathrm{R}} = \frac{1}{2}(1 - \beta_e) \qquad p_e^{\mathrm{L}} = \frac{1}{2}(1 + \beta_e) \,. \tag{3.3}$$

One can see the suppression of emitting right–handed electrons. Similarly, one can find the same suppression of emitting left–handed positrons.

Now let us assume that the probabilities of emitting left or right handed electron holds for any β decay process. This is not as artificial as may seem at a first glance. Having pure V–A theory and assuming massless neutrinos, these are produced exclusively as left handed chiral components, having negative helicity. Antineutrinos are also produced left handed, but for v spinors "helicity$=-$chirality", so they have a positive helicity. Electrons can be produced with both helicities, and the corresponding probability is given by (3.3). In general, one may postulate the following:

- Massless fermions are produced exclusively left handed
- Massless antifermions are produced exclusively right handed
- Massful fermions are produced left handed with the probability $\frac{1}{2}(1+\beta_f)$
- Massful antifermions are produced left handed with the probability $\frac{1}{2}(1-\beta_f)$

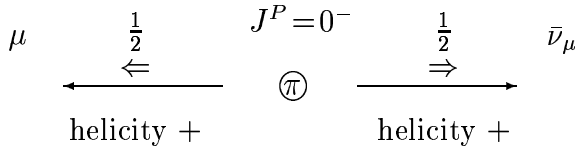

Figure 3.1: Illustration of the spin conservation in the pion decay

Specially, we will apply this on the pion decay. As the antineutrino is right–handed (positive helicity) and the pion is a spin zero particle, also electron has to be produced as a right–handed in order to hold the angular momentum conservation, i.e. just in the suppressed spin configuration!

According to assumptions made above, one would expect the ration of decay rates to be roughly equal to

$$\frac{\Gamma(\pi \to e\,\nu_e)}{\Gamma(\pi \to \mu\,\nu_\mu)} = \frac{p_e^{\mathrm{R}}}{p_\mu^{\mathrm{R}}}\,\frac{\mathrm{LIPS}_2(\pi \to e\,\nu_e)}{\mathrm{LIPS}_2(\pi \to \mu\,\nu_\mu)} = \frac{1-\beta_e}{1-\beta_\mu}\,\frac{m_\pi^2 - m_e^2}{m_\pi^2 - m_\mu^2}\,.$$

Of course, this is just a heuristic expression, not having computed the process properly, we do not know the precise dynamics, but we may just hope to get an improved result than just taking into account the phase space. Evaluating the velocities

$$\beta_f = \frac{p_f^*}{E_f^*} = \frac{p_f^*}{\sqrt{p_f^{*\,2} + m_f^2}} \qquad \text{with} \qquad p_f^* = \frac{m_\pi^2 - m_f^2}{2m_\pi}$$

and performing the algebra we arrive at

$$\frac{\Gamma(\pi \to e\,\nu_e)}{\Gamma(\pi \to \mu\,\nu_\mu)} = \frac{m_e^2}{m_\mu^2}\,\left(\frac{m_\pi^2 - m_e^2}{m_\pi^2 - m_\mu^2}\right)^2\,,$$

which is actually the same expression as will be derived in the following section being in a good agreement with experiment! (see below)

3.2 More proper explanation

We may well describe the process with a Fermi–like Lagrangian of V–A currents

$$\mathcal{L}_{\mathrm{int}}^{\pi} = -\frac{G_{\mathrm{F}}}{\sqrt{2}}\,\cos\theta_{\mathrm{C}}\,\left[\,\bar{l}\gamma_\rho(1-\gamma_5)\nu_l\right]\,\left[\bar{u}\gamma^\rho(1-\gamma_5)d\,\right]\,,$$

where the Cabbibo angle θ_{C} accounts for the "quark mixing" amplitude. The problem is the computing of the matrix element of the quark part with the pion state, as this is not known being a reflection of non-perturbative QCD.

As the first simplification, one can insert a complete set of projection operators to all states between the leptonic and hadronic part of the Lagrangian; however, of this infinite sum only

the vacuum projection survives (creation and annihilation operators in final and initial states meet with those in Lagrangian, and thus we are left only with the vacuum):

$$\langle l^-|\langle\bar{\nu}_l|\,\mathcal{L}^{\pi}_{\rm int}\,|\pi^-\rangle = -\frac{G_{\rm F}}{\sqrt{2}}\,\cos\theta_{\rm C}\,\langle l^-|\langle\bar{\nu}_l|\,\bar{l}\gamma_\rho(1-\gamma_5)\nu_l\,|0\rangle\times\langle 0|\,\bar{u}\gamma^\rho(1-\gamma_5)d\,|\pi^-\rangle\,.$$

Thus we have separated the quark and lepton matrix elements. The quark–pion matrix element must "match" the leptonic one in the sense that $\mathcal{M}_{fi}$ has to be a Lorentz scalar. Therefore, we need a fourvector index to be contracted with the leptonic part, and having in game only the pion fourvector q, one can write the most general Lorentz covariant contribution of the hadronic part as

$$q^\rho F_\pi(q^2)\,.$$

As we deal with an on–shell pion decay, $q^2 = m_\pi^2$, so the formfactor F_π is simply a constant, which is often redefined as $F_\pi = f_\pi\sqrt{2}$ and is a fundamental parameter describing the spontaneous breakdown of chiral symmetry.
Actually, pion is a pseudoscalar particle, with the intrinsic parity quantum number being -1, and making $\mathcal{M}_{fi}$ a Lorentz scalar, one needs the axial current in Lagrangian to get a nontrivial contribution (two quantities will change sign under a parity transformation, so the overall sign remains unchanged). The vector part would have to be coupled to a pseudovector, which, however, cannot be made from the fourvector q.
Fortunately, the ratio of decay widths

$$\frac{\Gamma(\pi\to e\,\nu_e)}{\Gamma(\pi\to\mu\,\nu_\mu)}$$

does not depend on the constant f_π, so we may compute the corresponding theoretical prediction. Assigning the fourmomentum of pion, lepton and the antineutrino as q, p, k and using basic Feynman rules we get

$$\mathcal{M}_{fi} = -G_{\rm F}\,\cos\theta_{\rm C}\,f_\pi q_\rho v(k)\gamma^\rho(1-\gamma_5)u(p)\,.$$

Inserting $q = p + k$ and using Dirac equations

$$(\not{p} - m_l)u(p) = 0 \qquad \not{k}\,v(k) = 0$$

we obtain

$$\mathcal{M}_{fi} = -G_{\rm F}\,\cos\theta_{\rm C}\,f_\pi\,m_l\,v(k)\gamma^\rho(1-\gamma_5)u(p)\,.$$

Squaring the expression and summing over all lepton spins we arrive at

$$\begin{aligned}\overline{|\mathcal{M}_{fi}|^2} &= G_{\rm F}^2\,\cos^2\theta_{\rm C}\,f_\pi^2\,m_l^2\,{\rm Tr}[\,\not{k}\,(1+\gamma_5)(\not{p}+m_l)(1-\gamma_5)]\\ &= G_{\rm F}^2\,\cos^2\theta_{\rm C}\,f_\pi^2\,m_l^2\,{\rm Tr}[\,\not{k}\not{p} - \not{k}\gamma_5\not{p}\gamma_5]\\ &= 8G_{\rm F}^2\,\cos^2\theta_{\rm C}\,f_\pi^2\,m_l^2\,(k.p)\end{aligned}$$

As $q^2 = (k+p)^2 = k^2 + 2k.p + p^2 = m_l^2 + 2k.p$, we have finally

$$\overline{|\mathcal{M}_{fi}|^2} = 4G_{\rm F}^2\,\cos^2\theta_{\rm C}\,f_\pi^2\,m_l^2(m_\pi^2 - m_l^2)\,. \tag{3.4}$$

Now the decay width is proportional to the phase space

$$\Gamma(\pi\to l\,\nu_l) \propto {\rm LIPS}_2(\pi\to l\,\nu_l)\times\overline{|\mathcal{M}_{fi}|^2}\,,$$

so according to (3.2) and (3.4) we get the prediction

$$\frac{\Gamma(\pi \to e\,\nu_e)}{\Gamma(\pi \to \mu\,\nu_\mu)} = \frac{m_e^2}{m_\mu^2}\left(\frac{m_\pi^2 - m_e^2}{m_\pi^2 - m_\mu^2}\right)^2$$

which, when evaluated for $m_\pi \doteq 139.6\,\mathrm{GeV}$, $m_\mu \doteq 105.6\,\mathrm{GeV}$, $m_\pi \doteq 0.5\,\mathrm{MeV}$, gives the value

$$\frac{\Gamma(\pi \to e\,\nu_e)}{\Gamma(\pi \to \mu\,\nu_\mu)} = 1.28 \times 10^{-4}$$

in a good agreement with the experimental value (3.1).
Further discussions can again be found in ([7]).

Chapter 4

Kaons

(under construction:-)

4.1 Decay modes, parity violation

At first, people thought kaons were an isospin triplet, but they turned out to be two doublets

$$K^0(d\bar{s}) \qquad K^+(u\bar{s})$$

$$K^-(\bar{s}) \qquad \bar{K}^0(s\bar{d})$$

To get some help in order to remember what is K^0 and $\bar{K}^0$ one can remember that K^0 $(d\bar{s})$ is being born with Λ^0 (uds)

$$p + \pi^- \to K^0 + \Lambda^0$$

Hadronic decays of kaons

$$K \to 3\pi$$

$$K \to 2\pi$$

clearly violate parity (therefore, parity of K mesons cannot be determined from these decays) as first mode would imply $P_K = P_\pi^3$, whereas the latter $P_K = P_\pi^2$ Semileptonic decays make a distinction between K^0 and $\bar{K}^0$:

$$K^0 \to l^+\nu_l + \pi^-$$

$$\bar{K}^0 \to l^-\bar{\nu}_l + \pi^+$$

being a manifestation of the rule $\Delta S = \Delta Q$ and are used in measuring the CP violation parameters.

4.2 K^0–$\bar{K}^0$ mixing

As parity is violated, at first it was thought that combined CP symmetry could hold. K^0 and $\bar{K}^0$ are strong interaction eigenstates, they can be transformed to each other by the C operation and have opposite (and defined) strangenesses. Having no weak interaction, they would be degenerate in masses. However, physical states with well defined masses are a linear combinations of K^0 and $\bar{K}^0$ and the degeneracy in masses is lost due to weak interaction.

Also, physical states have to be CP eigenstates. As $P|K^0\rangle = -|K^0\rangle$, we can define the phase convention as

$$CP|K^0\rangle = |\bar{K}^0\rangle$$

Using the trick

$$|K^0\rangle = \frac{1}{2}(|K^0\rangle + |\bar{K}^0\rangle) + \frac{1}{2}(|K^0\rangle - |\bar{K}^0\rangle)$$

we can recast

$$|K_S^0\rangle = \frac{1}{\sqrt{2}}(|K^0\rangle + |\bar{K}^0\rangle)$$

$$|K_L^0\rangle = \frac{1}{\sqrt{2}}(|K^0\rangle - |\bar{K}^0\rangle)$$

and inversely

$$|K^0\rangle = \frac{1}{\sqrt{2}}(|K_S^0\rangle + |K_L^0\rangle)$$

$$|\bar{K}^0\rangle = \frac{1}{\sqrt{2}}(|K_S^0\rangle - |K_L^0\rangle)\,.$$

The important thing is that states $|K_S^0\rangle$ and $|K_L^0\rangle$ are built so as

$$CP|K_S^0\rangle = |K_S^0\rangle$$

$$CP|K_L^0\rangle = -|K_L^0\rangle\,.$$

As the CP eigenvalues for 3π and 2π systems are $CP(3\pi) = -1$ and $CP(2\pi) = 1$, following decays are possible

$$|K_S^0\rangle \to 3\pi$$

$$|K_L^0\rangle \to 2\pi\,,$$

whereas these are **not**

$$|K_S^0\rangle \to 2\pi$$

$$|K_L^0\rangle \to 3\pi\,.$$

As the available phase space is larger in the case of two pions in the final state, the corresponding partial decay width is smaller causing $|K_S^0\rangle$ to be short–lived and $|K_L^0\rangle$ a long–lived when compared to each other (experimentally $c\tau_S = 2.68\text{cm}$, $c\tau_S = 15.51\text{m}$).

Let us now suppose we have produced a beam of K^0 mesons. Soon, the short–lived component will vanish leaving the long–lived, which, however, includes both K^0 and $\bar{K}^0$! As we shall see, one actually observes K^0–$\bar{K}^0$ oscillations in the originally pure K^0 beam.

In order to distinguish K^0 and $\bar{K}^0$ we shall make use of semileptonic decays of kaons and will measure the probability

$$|\langle l^+\nu_l\pi^-|K^0(t)\rangle|^2$$

assuming that system was prepared in pure K^0 in $t=0$.
We know the evolution of mass eigenstates under the overall Hamiltonian

$$|K_S^0(t)\rangle = e^{-im_S t - \Gamma_S t/2}|K_S^0\rangle$$

$$|K_L^0(t)\rangle = e^{-im_L t - \Gamma_L t/2}|K_L^0\rangle\,,$$

so the evolution of $|K^0(t)\rangle$ is simply

$$|K^0(t)\rangle = \frac{1}{\sqrt{2}}\left(e^{-im_S t-\Gamma_S t/2}|K^0_S\rangle + e^{-im_L t-\Gamma_L t/2}|K^0_L\rangle\right) .$$

Now only K^0 can undergo the transition into the final state with the positively charged lepton, so

$$\begin{aligned}|\langle l^+\nu_l\pi^-|K^0(t)\rangle|^2 &= \left|\langle l^+\nu_l\pi^-|\frac{1}{\sqrt{2}}\left(e^{-im_S t-\Gamma_S t/2}|K^0_S\rangle + e^{-im_L t-\Gamma_L t/2}|K^0_L\rangle\right)\right|^2 \\ &= \left|\langle l^+\nu_l\pi^-|\frac{1}{2}\left[e^{-im_S t-\Gamma_S t/2}(|K^0\rangle + |\bar{K}^0\rangle) + e^{-im_L t-\Gamma_L t/2}(|K^0\rangle - |\bar{K}^0\rangle)\right]\right|^2 \\ &= \frac{1}{4}\left|e^{-im_S t-\Gamma_S t/2} + e^{-im_L t-\Gamma_L t/2}\right|^2 ,\end{aligned}$$

so finally

$$|\langle l^+\nu_l\pi^-|K^0(t)\rangle|^2 = \frac{1}{4}\Big[e^{-\Gamma_S t} + e^{-\Gamma_L t} + e^{-(\Gamma_S+\Gamma_L)t/2}2\cos(m_S - m_L)t\Big]$$

and similarly

$$|\langle l^-\bar{\nu}_l\pi^+|K^0(t)\rangle|^2 = \frac{1}{4}\Big[e^{-\Gamma_S t} + e^{-\Gamma_L t} - e^{-(\Gamma_S+\Gamma_L)t/2}2\cos(m_S - m_L)t\Big] .$$

The quantity that can be experimentally well tested is the asymmetry in number of observed positive and negative leptons

$$A(t) = \frac{N(l^+) - N(l^-)}{N(l^+) + N(l^-)} ,$$

for which our calculations give the prediction

$$A(t) = \frac{e^{-(\Gamma_S+\Gamma_L)t/2}\cos(m_S - m_L)t}{\frac{1}{2}\left(e^{-\Gamma_S t} + e^{-\Gamma_L t}\right)} .$$

The result is plotted using the experimental value of $m_S - m_L \doteq 3.49 \pm 0.006)\times 10^{-12}\,\mathrm{MeV}$ and above mentioned widths in Figures 4.1 and 4.2

4.3 CP violation

4.4 Problem of neutral kaon decay, GIM mechanism

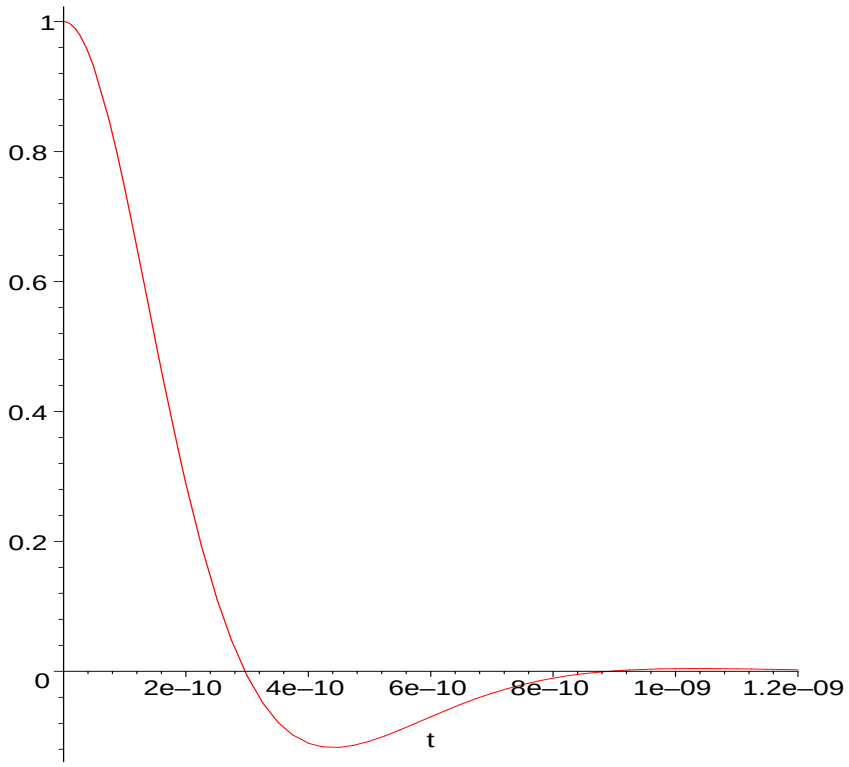

Figure 4.1: Asymmetry coefficient as a function of time (in s) demonstrating the K^0–$\bar{K}^0$ mixing.

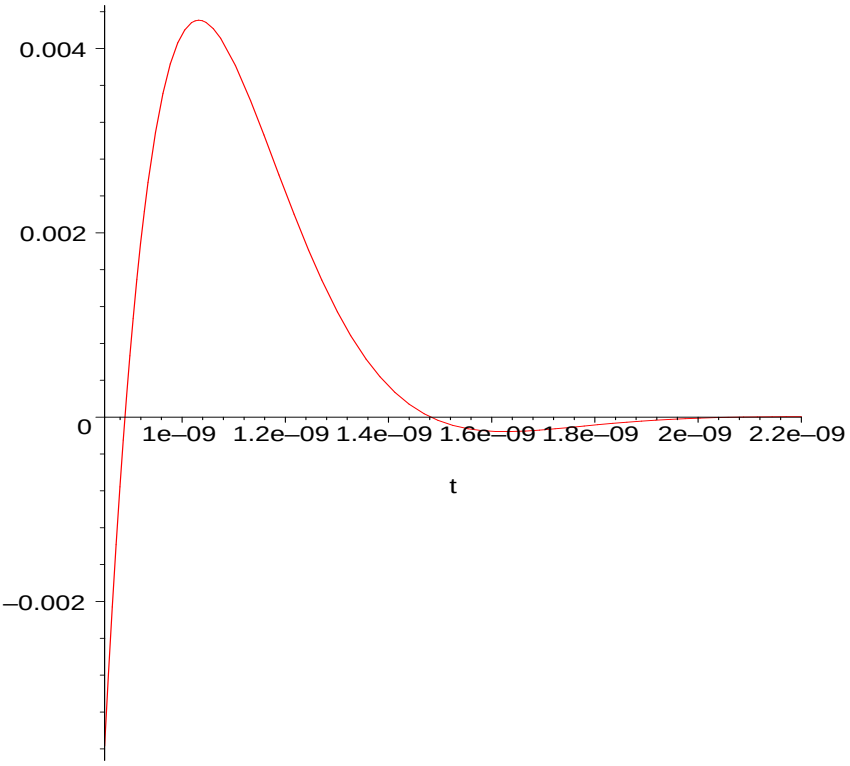

Figure 4.2: Detail of the previous plot, zoomed in the y axis for larger t.

Chapter 5

η and η' mesons

(under construction:-)

5.1 G–Parity and η meson decays

G–Parity is a combination of Parity and a reflection in the isospin space

$$G \equiv C \exp\left(i\pi I_2\right).$$

It is an approximate invariant in strong and electromagnetic processes. For example (Weinberg, Phys. Rev. **112** (1958), 1345) for nucleon doublet and pion triplet

$$G\psi_N G^{-1} = i\tau_2 \psi_N \qquad G\phi_\pi G^{-1} = -\phi_\pi$$

π	$J^{GP} = 0^{--}$
η	$J^{GP} = 0^{+-}$

Table 5.1: G–parity of π and η

Therefore, for strong η meson decays

- $\eta \to \pi\pi$ is forbidden due to parity conservation
- $\eta \to \pi\pi\pi$ is suppressed due to G–parity conservation
- $\eta \to \pi\pi\pi\pi$ is forbidden due to kinematics (except for the case where all pions are neutral, but is forbidden by CP conservation)

Actually, all strong modes of η are suppressed in the lowest order making η's lifetime about five orders of magnitude longer than for example of the ρ meson ($m_\eta \doteq 547\,\mathrm{MeV}$, $\Gamma_\eta \doteq 1.18\,\mathrm{keV}$, $\tau_\eta \doteq 5.7 \times 10^{-19}$ s, whereas $m_\rho \doteq 771\,\mathrm{MeV}$, $\Gamma_\rho \doteq 150\,\mathrm{MeV}$, $\tau_\rho \doteq 4.4 \times 10^{-24}$ s). Decays to three pions actually do occur, but as a higher order process (isospin symmetry is broken).

The largest branching ratio is $\eta \to 2\gamma$ and $\eta \to 3\pi^0$.

5.2 η and η' mixing

States with the same IJ^P and additive quantum numbers (strangeness...) can mix (if they are in addition charge conjugate eigenstates, the must also have the same value of C). Specially, the zero isospin member of the pseudoscalar meson octet η_8 mixes with the singlet η_1 producing η and η'. Similar mixing appears to produce ω and ϕ in vector mesons.

$$\eta_1 = \frac{1}{\sqrt{3}}|u\bar{u} + d\bar{d} + s\bar{s}\rangle$$

$$\eta_8 = \frac{1}{\sqrt{6}}|u\bar{u} + d\bar{d} - 2s\bar{s}\rangle$$

$$\eta = \eta_8 \cos\theta_P - \eta_1 \sin\theta_P$$

$$\eta' = \eta_8 \sin\theta_P + \eta_1 \cos\theta_P$$

$$\phi = \omega_8 \cos\theta_V - \omega_1 \sin\theta_V$$

$$\omega = \omega_8 \sin\theta_V + \omega_1 \cos\theta_V$$

Approximate values for these mixing angles are (experimental results) $\theta_P \approx 20°$, $\theta_V \approx 35°$.

Chapter 6

Discovery of the c quark – November revolution and J/ψ

(under construction:-)

In November 1974, the world of particle physics was astonished by two independent discoveries of a very narrow new particle with a mass of approximately 3.1 GeV. One experiment was a proton machine with a Be target, the other a e^+e^- collider. Thus, J/ψ was found in two complementary processes. Citing from works **??**, **??** we get to know following interesting facts:

Samuel Ting et al:

- **We report an observation of a heavy particle J, with mass $m = 3.1\,\mathrm{GeV}$ and width approximately zero. The observation was made from the reaction $p + Be \to e^+e^- + X$ by measuring the e^+e^- mass spectrum at the Brookhaven National Laboratory's 30 GeV alternating-gradient synchrotron.**
- To ensure that he observed peak is indeed a real particle ($J \to e^+e^-$) many experimental checks were made. We list seven examples ...
- The most striking feature of J is the possibility that it may be one of the theoretically suggested charmed particles or a a's or Z_0's, etc.
- It is also important to note the absence of an e^+e^- continuum, which contradicts the predictions of parton models [an improved version of the theory is not in contradiction with the data].

Burton Richter et al, Stanford Linear Accelerator Center (SLAC) – Lawrence Berkeley Laboratory magnetic detector at the SLAC electron–positron storage ring SPEAR.

- **We have observed a very sharp peak in the cross section for $e^+e^- \to$ hadrons, e^+e^- and possibly $\mu^+\mu^-$ at a centre-of-mass energy of $3.105 \pm 0.005\,\mathrm{GeV}$. The upper limit to the full width at half maximum is 1.3 MeV ... we suggest naming this structure $\psi(3105)$:**
- The cross section for hadron production at the peak of the resonance is ≥ 2300 nb, an enhancement of about 100 times the cross section outside the resonance. The large mass, large cross section, and narrow width of this structure are entirely unexpected.

- The 3.2 GeV results reproduced, the 3.3 GeV measurement showed no enhancement, but the 3.1 GeV measurements were internally inconsistent – six out of eight runs giving a low cross section and two runs giving a factor of 3 to 5 higher cross section. This pattern could have been caused by a very narrow resonance at an energy slightly larger then the nominal 3.1 GeV setting of the storage ring, the inconsistent 3.1 GeV cross sections then being caused by setting errors in the ring energy.
- It is difficult to understand how, without involving new quantum numbers or selection rules, a resonance in this state which decays to hadrons could be so narrow.

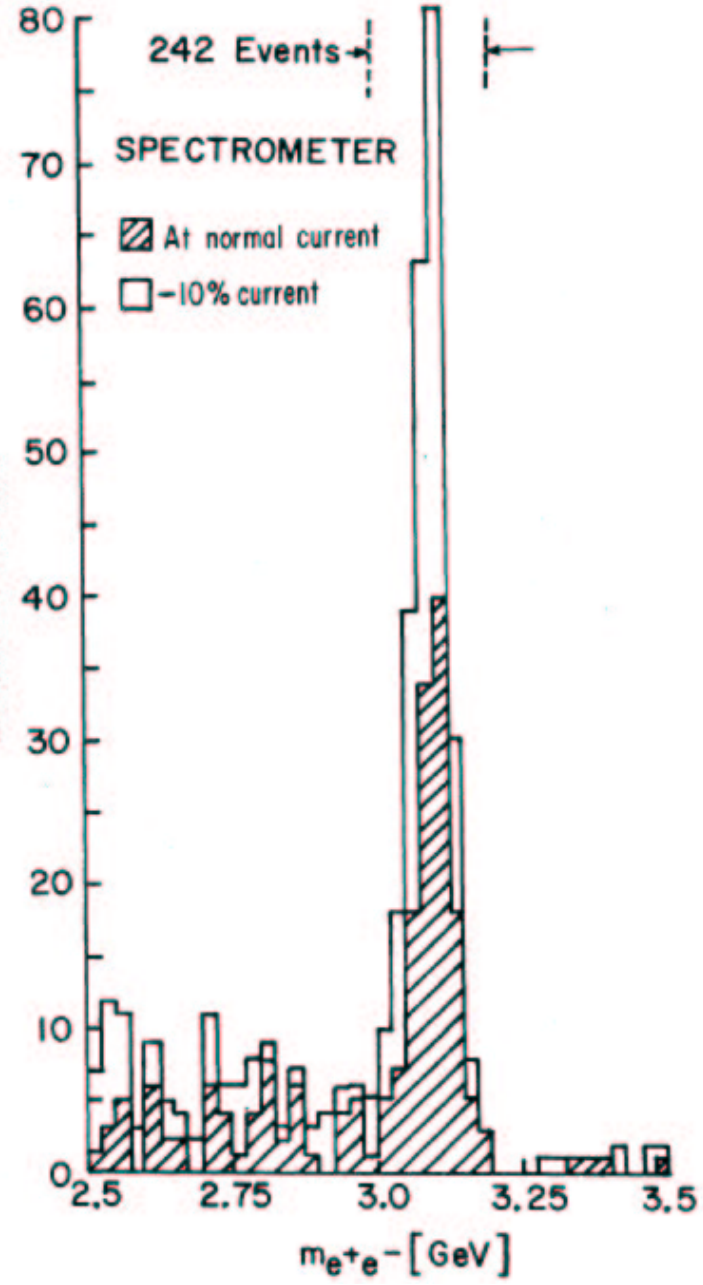

FIG. 2. Mass spectrum showing the existence of J. Results from two spectrometer settings are plotted showing that the peak is independent of spectrometer currents. The run at reduced current was taken two months later than the normal run.

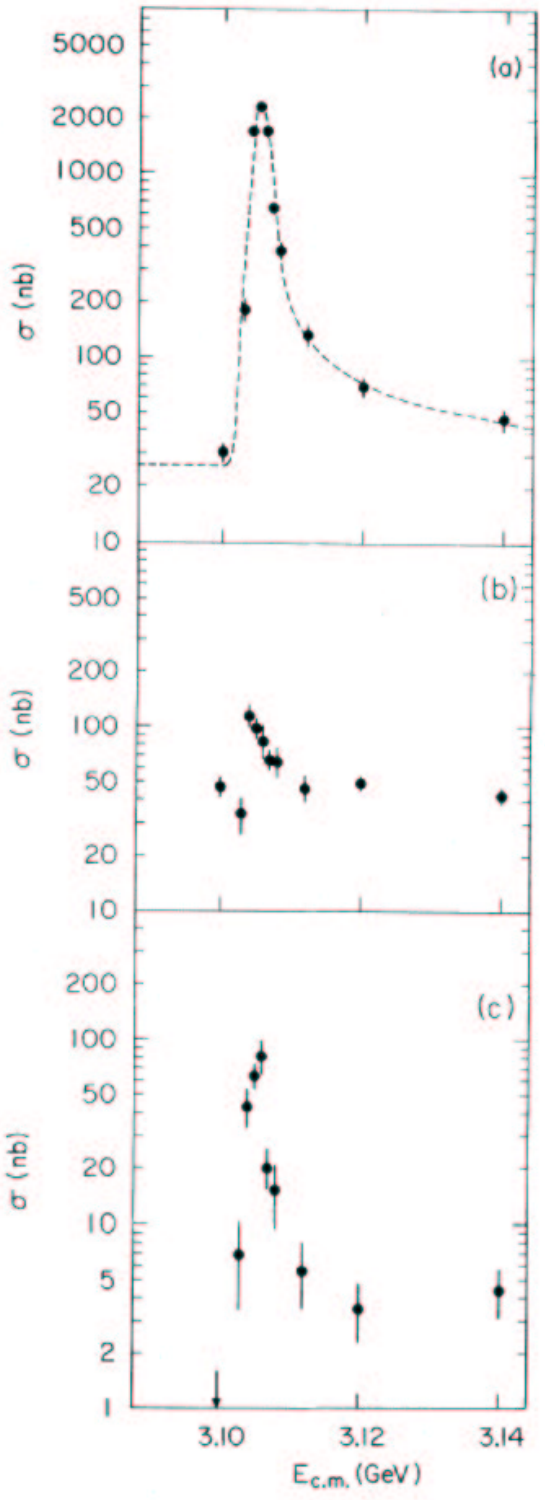

FIG. 1. Cross section versus energy for (a) multihadron final states, (b) e^+e^- final states, and (c) $\mu^+\mu^-$, $\pi^+\pi^-$, and K^+K^- final states. The curve in (a) is the expected shape of a δ-function resonance folded with the Gaussian energy spread of the beams and including radiative processes. The cross sections shown in (b) and (c) are integrated over the detector acceptance. The total hadron cross section, (a), has been corrected for detection efficiency.

Figure 6.1: Evidence for the J and ψ resonances

Chapter 7

Additive quark model

π^0 and ρ mesons are combinations of $\frac{1}{\sqrt{2}}|u\bar{u} - d\bar{d}\rangle$

$$\omega = \frac{1}{\sqrt{2}}|u\bar{u} + d\bar{d}\rangle$$

$$\eta_1 = \frac{1}{\sqrt{3}}|u\bar{u} + d\bar{d} + s\bar{s}\rangle$$

$$\eta_8 = \frac{1}{\sqrt{6}}|u\bar{u} + d\bar{d} - 2s\bar{s}\rangle$$

Chapter 8

$e^+e^- \to$ hadrons, evidence for colour

A production of hadrons from the e^+e^- annihilations in the second order of a perturbation theory is possible via the exchange of a virtual photon (or Z and perhaps Higgs at higher energies) giving a birth of a quark–antiquark pair. Of course, this is possible only above the threshold $m_q \leq \sqrt{s}$.

Expressions for cross sections are of the same form for $\mu^+\mu^-$ and $q\bar{q}$ production with the only difference in the charge square of particles involved. Cross section formulæ involve threshold factors (coming from the dynamics and phase space) of the type ([6], pg. 767)

$$\left(1 + \frac{2m_f^2}{s}\right)\sqrt{1 - \frac{4m_f^2}{s}}\,.$$

However, these quickly vanish when increasing energy over the threshold and in the expression

$$R(s) \equiv \frac{\sigma(e^+e^- \to \text{hadrons})}{\sigma(e^+e^- \to \mu^+\mu^-)}$$

only the charge factors will remain giving the prediction

$$R(s) = \sum_q Q_q^2\,,$$

where summed over all quarks available at the given energy.

One may ask, why we normalise the hadron production cross section on the $\mu^+\mu^-$ production and not the e^+e^-. The answer is simple: the latter one diverges in the similar way as the Rutherford formula (will be updated).

This ratio is experimentally measured as a ration of hadron and pure $\mu^+\mu^-$ events in e^+e^- collisions. If quarks have some additional degrees of freedom (presumably associated with colour, therefore denoting as N_C), the corresponding prediction is just grater by this factor

$$R(s) = N_\mathrm{C} \sum_q Q_q^2\,.$$

Assuming quark charges $+2/3$ for u, c, t and $-1/3$ for d, s, b, then predictions for R are as seen in Table 14.1. In case of three colours $N_\mathrm{C} = 3$, the predictions are in a good agreement with experiment giving the support to the idea of three additional degrees of freedom for quarks, i.e. the colour (see Table 8.2).
For further details see [6], pg. 764–770.

quarks in game	prediction for R
$u,\ d,\ s$	$R = \frac{6}{9} N_{\mathrm{C}} = 0.\bar{6} N_{\mathrm{C}}$
$u,\ d,\ s,\ c$	$R = \frac{10}{9} N_{\mathrm{C}} = 1.\bar{1} N_{\mathrm{C}}$
$u,\ d,\ s,\ c,\ b$	$R = \frac{11}{9} N_{\mathrm{C}} = 1.\bar{2} N_{\mathrm{C}}$

Table 8.1: R values for different quarks in game

quarks in game	prediction for R, $N_{\mathrm{C}} = 3$
$u,\ d,\ s$	$R = \frac{6}{9} N_{\mathrm{C}} = 2$
$u,\ d,\ s,\ c$	$R = \frac{10}{9} N_{\mathrm{C}} = 3.\bar{3}$
$u,\ d,\ s,\ c,\ b$	$R = \frac{11}{9} N_{\mathrm{C}} = 3.\bar{6}$

Table 8.2: R values for different quarks in game in case of tree colours.

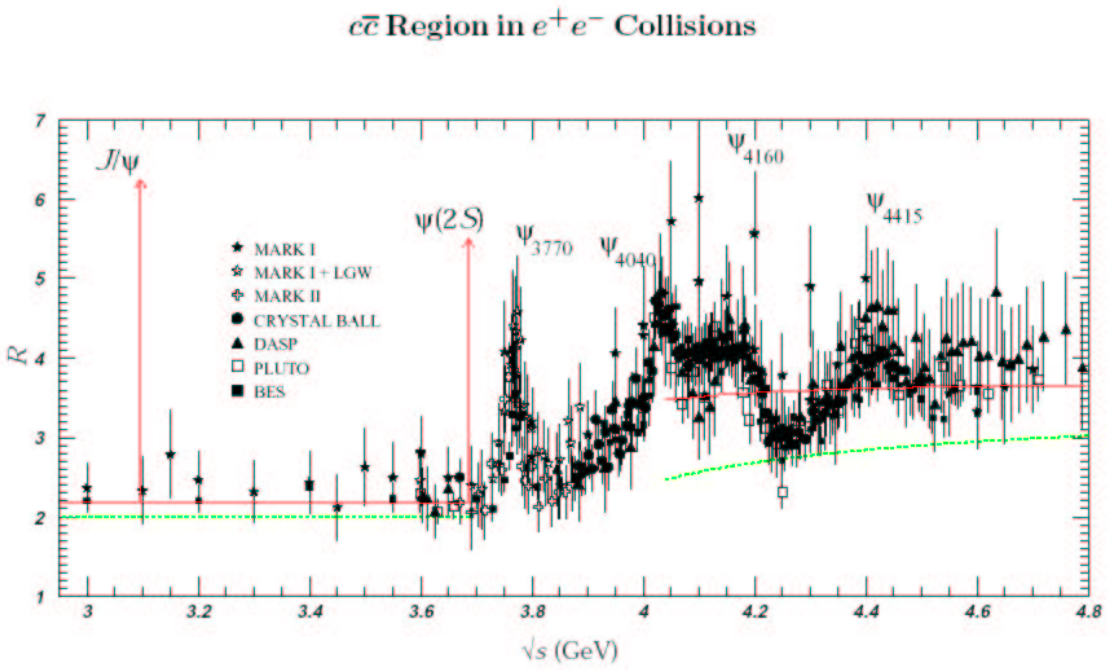

Figure 39.8: The ratio $R = \sigma(e^+e^- \to hadrons)/\sigma(e^+e^- \to \mu^+\mu^-$, QED-simple pole) in the $c\bar{c}$ region. (See the caption for Figs. [39.6–39.7]). **Note:** The experimental shapes of J/ψ and $\psi(2S)$ resonances are dominated by machine energy spread and are not shown.

Figure 8.1: R in the J/ψ region, taken from the Particle Data Group ([11])

Chapter 9

Symmetries

(under construction:-)

9.1 Parity

Chapter 10

Standard Model

The standard model[1] (SM) of electroweak interactions is in excellent agreement with present-day experimental data (LEPII, Tevatron, SLD) [16]. The SM was formulated by S. Glashow, A. Salam and S. Weinberg [17] in 1960s and a proof of its perturbative renormalisability was invented by G. 't Hooft in 1971 [18]. The SM involves 17 particles: six leptons (e, ν_e, μ, ν_μ, τ, ν_τ), six quarks (u, d, s, c, b, t), three intermediate vector bosons ($W^\pm$, Z), photon (γ) and scalar Higgs boson (H). Leptons and quarks are regarded as constituents of the "matter". Intermediate bosons and the photon are carriers of electroweak forces. The Higgs boson is related to the mechanism of generation of particle masses and plays thus an important role in theoretical construction of SM. However, it has not been experimentally detected yet.

In this chapter we present a brief overview of the SM formulation. Further details can be found in many textbooks (in particular, I relied mostly on [7]).

10.1 Basic principles

The electroweak SM is a gauge theory with $SU(2) \times U(1)$ symmetry, which is "spontaneously broken" down to the electromagnetic $U(1)$; Electroweak symmetry breaking is the so-called Higgs mechanism, which produces particle masses. Let us first summarise briefly the field contents of SM. The basic building blocks for elementary fermions are the left-handed $SU(2)$ doublets

$$L^{(e)} = \begin{pmatrix} \nu_{eL} \\ e_L \end{pmatrix}, \qquad L^{(\mu)} = \begin{pmatrix} \nu_{\mu L} \\ \mu \end{pmatrix}, \qquad L^{(\tau)} = \begin{pmatrix} \nu_{\tau L} \\ \tau \end{pmatrix},$$
$$L^{(d)} = \begin{pmatrix} u_L \\ d_L \end{pmatrix}, \qquad L^{(s)} = \begin{pmatrix} c_L \\ s_L \end{pmatrix}, \qquad L^{(b)} = \begin{pmatrix} t_L \\ b_L \end{pmatrix}$$

and right-handed singlets

$$\begin{array}{cccccc} e_R, & \mu_R, & \tau_R, & \nu_{eR}, & \nu_{\mu R}, & \nu_{\tau R}, \\ u_R, & d_R, & c_R, & s_R, & t_R, & b_R \end{array}$$

(where $e_L = \frac{1}{2}(1-\gamma_5)e$, $e_R = \frac{1}{2}(1+\gamma_5)e$ etc.). Here we have included right-handed neutrino fields, just to indicate that massive neutrinos could be incorporated in SM in a natural way; nevertheless, in what follows we will drop these altogether, since they do not play any role in our considerations. In general, the fields shown above do not correspond to mass eigenstates; in order to get particles with definite masses, one has to diagonalise appropriate mass ma-

[1] This review is taken from the diploma thesis by Miro Kladiva ([9]) with his personal courtesy and support

trices (note that in the simplified model with massless neutrinos there is no need for such a diagonalisation for leptons).

Intermediate vector bosons and the photon correspond to the Yang-Mills fields associated with the four generators of the local $SU(2) \times U(1)$ symmetry. Finally, for implementing the Higgs mechanism one needs a complex scalar doublet

$$\Phi = \begin{pmatrix} \varphi^+ \\ \varphi^0 \end{pmatrix} \tag{10.1}$$

Now we are going to construct the SM Lagrangian. For simplicity we shall consider only one lepton family, e.g. (ν_e, e). The gauge invariant term involving leptons and Yang-Mills fields can be written as

$$\mathcal{L}_{\text{lepton}} = i\bar{L}\gamma^\mu D_\mu^{(L)} L + i\bar{e}_R \gamma^\mu D_\mu^{(R)} e_R \tag{10.2}$$

where $D_\mu^{(L)}$ and $D_\mu^{(R)}$ are covariant derivatives

$$\begin{aligned} D_\mu^{(L)} &= \partial_\mu - igA_\mu^a \frac{\tau^a}{2} - ig' Y_L B_\mu \\ D_\mu^{(R)} &= \partial_\mu - ig' Y_R^{(e)} B_\mu \end{aligned} \tag{10.3}$$

Here the τ_i are Pauli matrices, A_μ^a and B_μ stand for the Yang-Mills gauge fields and the Y_L and Y_R denote the "weak hypercharge" (that characterises the transformation properties of the corresponding field under the $U(1)$ subgroup). Note that the relevant values of the Y are given by

$$Q = T_3 + Y$$

with Q and T_3 denoting the electric charge and third component of "weak isospin" respectively (for example, $Q = -1$ and $T_3 = -1/2$ for left-handed electron, so that $Y_L = -1/2$).

To incorporate the kinetic terms for Yang-Mills fields in gauge invariant way, one has to introduce the form

$$\mathcal{L}_{\text{gauge}} = -\frac{1}{4} F_{\mu\nu}^a F^{a\mu\nu} - \frac{1}{4} G_{\mu\nu} G^{\mu\nu} \tag{10.4}$$

where

$$\begin{aligned} F_{\mu\nu}^a &= \partial_\mu A_\nu - \partial_\nu A_\mu + g\varepsilon_{abc} A_\mu^a A_\nu^b \\ G_{\mu\nu} &= \partial_\mu B_\nu - \partial_\nu B_\mu \end{aligned} \tag{10.5}$$

with e_{abc} being the three-dimensional Levi-Civita symbol. It should be noticed that, apart from kinetic terms, the Lagrangian (10.4) involves also some specific self-interactions of Yang-Mills fields.

To implement the Higgs mechanism, one adds the Lagrangian

$$\mathcal{L}_{\text{Higgs}} = \left(D^\mu \Phi\right)^\dagger D_\mu \Phi - \lambda \left(\Phi^\dagger \Phi - \frac{v^2}{2} \right)^2 \tag{10.6}$$

where Φ is the doublet (10.1) and D_μ stands for the covariant derivative

$$D_\mu = \partial_\mu - igA_\mu^a \frac{\tau_a}{2} - \frac{i}{2} g' B_\mu \tag{10.7}$$

The λ appearing in (10.6) is a positive (dimensionless) coupling constant and v is a parameter with dimension of mass. Note that the form of the "potential" involving the λ and v is responsible for the spontaneous breakdown of $SU(2)$ symmetry — this leads to appearance of three

Goldstone bosons, before introducing the Yang-Mills fields (i.e. the local gauge symmetry). It is convenient to employ the parametrisation

$$\Phi = \exp\Big(\frac{i}{v}\pi^a(x)\tau^a\Big)\begin{pmatrix}0\\ \frac{1}{\sqrt{2}}\big(v+H(x)\big)\end{pmatrix} \tag{10.8}$$

where π^a represent the Goldstone bosons and H denotes another real scalar — the Higgs boson. In the $SU(2)\times U(1)$ gauge theory, the original Goldstone boson fields are unphysical as they can be removed by means of appropriate $SU(2)$ gauge transformation. This is tantamount to fixing a particular gauge, the so-called "unitary", or simply U-gauge. In such a gauge the Φ becomes

$$\Phi_U = \begin{pmatrix}0\\ \frac{1}{\sqrt{2}}\big(v+H(x)\big)\end{pmatrix} \tag{10.9}$$

Note that, there are also other useful gauge-fixing conditions, e.g. the R-gauges described in Section. After substituting the Φ_U into the Lagrangian (10.6), we obtain interaction terms involving H, A^a_μ, B_μ and also quadratic terms for these fields (they are due to the constant shift v in Φ_U). The diagonalisation of the quadratic form for Yang-Mills fields yields three massive and one massless combination of the A^μ_a, B_μ; of course the massless field corresponds to the photon. The three massive fields (denoted as $W^\pm_\mu$ and Z_μ respectively) represent intermediate bosons of weak interactions. Two of them are electrically charged and the third one is neutral (the charge assignments become clear when one considers the interactions with leptons). The explicit form of the physical vector fields can be written as

$$\begin{aligned} W^\pm_\mu &= \frac{1}{\sqrt{2}}\left(A^1_\mu \mp iA^2_\mu\right)\\ Z_\mu &= \cos\vartheta_{\rm w}\, A^3_\mu - \sin\vartheta_{\rm w}\, B_\mu\\ A_\mu &= \sin\vartheta_{\rm w}\, B_\mu + \cos\vartheta_{\rm w}\, A^3_\mu \end{aligned} \tag{10.10}$$

where $\vartheta_{\rm w}$ is so-called Weinberg angle (or weak mixing angle) defined by $\tan\vartheta_{\rm w} = g'/g$. The corresponding masses, including that of the Higgs boson, (originating in the Higgs-Goldstone potential) are

$$\begin{aligned} m_H^2 &= 2\lambda v^2\\ m_W &= \frac{1}{2}gv\\ m_Z &= \frac{1}{2}(g^2+g'^2)^{1/2}v\\ m_A &= 0 \end{aligned} \tag{10.11}$$

Notice that from (10.11) one gets immediately the famous relation

$$\frac{m_W}{m_Z} = \cos\vartheta_{\rm w} \tag{10.12}$$

which is now confirmed by experimental data with great accuracy (note that $\cos\vartheta_{\rm w}$ can be simply related to the electromagnetic coupling constant e and weak coupling constant g (10.17))

To generate lepton masses, one has to introduce an additional piece to the Lagrangian, namely the Yukawa coupling

$$\mathcal{L}_{\rm Yukawa} = -h_e\bar{L}\Phi e_R + \text{h.c.}^2 \tag{10.13}$$

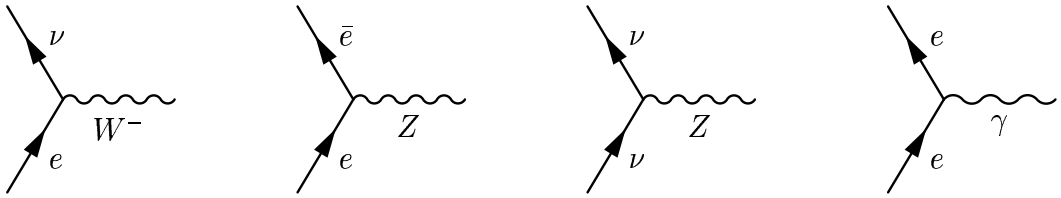

(a) (b) (c) (d)

Figure 10.1: The vector boson-lepton interactions

(where h.c. stands for Hermitian conjugation). The relevant mass term for electron is

$$m_e = \frac{1}{\sqrt{2}} h_e v$$

Note that in the quark sector of SM one has to start with more general Yukawa couplings, so as to incorporate the observed flavour mixing. This leads to diagonalisation of general quark mass matrices and to the subsequent appearance of the Cabibbo-Kobayashi-Maskawa mixing matrix in the interactions of W-bosons with quarks. Of course the same procedure is necessary if one wants to include masses of neutrinos and their possible mixing.

Thus, we obtain the SM Lagrangian in the form

$$\mathcal{L}_{\text{lepton}} + \mathcal{L}_{\text{gauge}} + \mathcal{L}_{\text{Higgs}} + \mathcal{L}_{\text{Yukawa}}$$

It's important to stress that there is a relation between the SM parameters and the fundamental parameter of the low-energy weak interaction physics — the Fermi constant G_F, namely

$$g^2 = \frac{8 G_F}{\sqrt{2}} m_W^2 \tag{10.14}$$

note that this also amounts to an expression for v,

$$v = \left(G_F \sqrt{2} \right)^{-\frac{1}{2}}$$

The nowadays value of G_F is

$$G_F = (1.16639 \pm 0.00001) \times 10^{-5}\ \text{GeV}^{-2} \tag{10.15}$$

In next sections we will discuss this Lagrangian in individual terms and relevant vertexes in Feynman diagrams.

10.2 Interactions of vector bosons with leptons

These interactions are obtained from $\mathcal{L}_{\text{lepton}}$ (see (10.2)). Substituting there the explicit form of the covariant derivatives (10.3) (and take into account the numerical values of the weak hypercharges), one has

$$\mathcal{L}_{\text{lepton}} = i \bar{L} \gamma^\mu \left(\partial_\mu - i g A_\mu^a \frac{\tau^a}{2} + \frac{i}{2} g' B_\mu \right) L + i \bar{e}_R \gamma^\mu \left(\partial_\mu + i g' B_\mu \right) e_R \tag{10.16}$$

Expressing the original gauge fields A^a_μ and B_μ in terms of the $W^\pm$, Z, A according to (10.10) we get two types of interactions. First, the "non-diagonal" part of the Lagrangian embodies the usual weak charged currents (CC) coupled to the $W^\pm$; this term is written as

$$\mathcal{L}_{\rm CC} = \frac{g}{2\sqrt{2}}\,\bar\nu\gamma^\mu(1-\gamma_5)e\,W^+_\mu + \text{h.c.}$$

Next, the "diagonal" part of the Lagrangian includes electromagnetic interaction

$$\mathcal{L}_{\text{el.-mag.}} = -\frac{gg'}{\sqrt{g^2+g'^2}}\,\bar e\gamma_\mu e\,A^\mu$$

where the coupling constant can be interpreted as the e (with $e^2/4\pi$ equal to the fine structure constant α). Note that one thus also obtains the relation

$$e = gg'/\sqrt{g^2+g'^2} = g\sin\vartheta_{\rm W} \tag{10.17}$$

The remaining part of the Lagrangian represents the interaction of a weak neutral current (NC) with the Z_μ, which becomes

$$\mathcal{L}_{\rm NC} = \frac{g}{2\cos\vartheta_{\rm W}}\left(\frac{1}{2}\bar\nu_\mu\gamma^\alpha(1-\gamma_5)\nu_\mu + \bar e\gamma^\alpha(v-a\gamma_5)e\right)Z_\alpha$$

with $v = -1/2 + 2\sin^2\vartheta_{\rm W}$ and $a = -1/2$.

10.3 Vector boson self-interactions

These couplings are obtained from the non-quadratic part of the Lagrangian (see (10.4)). It is easy to see that there are trilinear and quadrilinear terms in vector boson fields. For the trilinear part we have

$$\mathcal{L}_{WW\gamma} = -ie\left(A_\mu W^-_\nu \overleftrightarrow{\partial}^\mu W^{+\nu} + W^-_\mu W^+_\nu \overleftrightarrow{\partial}^\mu A^\nu + W^+_\mu A_\nu \overleftrightarrow{\partial}^\mu W^{-\nu}\right) \tag{10.18}$$

$$\mathcal{L}_{WWZ} = -ig\cos\vartheta_{\rm W}\left(Z_\mu W^-_\nu \overleftrightarrow{\partial}^\mu W^{+\nu} + W^-_\mu W^+_\nu \overleftrightarrow{\partial}^\mu Z^\nu + W^+_\mu Z_\nu \overleftrightarrow{\partial}^\mu W^{-\nu}\right) \tag{10.19}$$

These two Lagrangians are antisymmetric with respect to permutations of W^+_μ,W^-_μ, A_μ and contain derivatives of fields. Thus the Feynman rules for the corresponding two vertices are expressed by means of a function linear with respect to particle momenta

$$V_{\lambda\mu\nu}(k,p,q) = (k-p)_\nu g_{\lambda\mu} + (p-q)\lambda g_{\mu\nu} + (q-k)_\mu g_{\lambda\nu}$$

(the notation is shown in Fig. 10.2(a), with all momenta taken as outgoing), multiplied by appropriate coupling constants shown in (10.18) and (10.19). There are several useful properties of the function V, namely antisymmetry with respect to indices and permutation of momenta, and the so-called 't Hooft identity

$$p^\mu V_{\lambda\mu\nu} = (-q^2 g_{\lambda\nu} + q_\lambda q_\nu) - (-k^2 g_{\lambda\nu} + k_\lambda k_\nu) \tag{10.20}$$

widely used in practical calculations of Feynman diagrams.

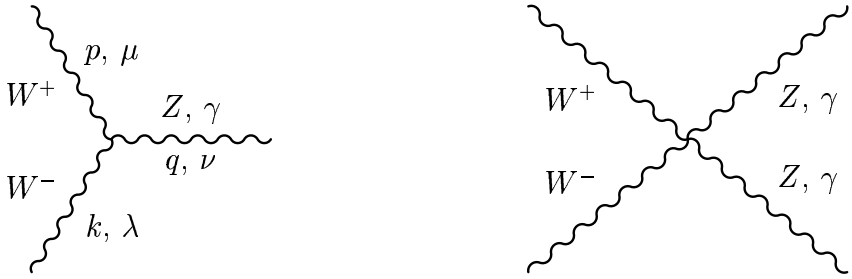

(a) (b)

Figure 10.2: Self-interactions of vector Bosons interactions

The quadrilinear interactions are richer, but do not contain the field derivatives. They can be obtained from the Lagrangian (10.4) in straightforward way; one gets

$$\mathcal{L}_{WWWW} = \frac{1}{2}g^2(W^-_\mu W^{-\mu} W^+_\nu W^{+\nu} - W^-_\mu W^{+\mu} W^-_\nu W^{+\nu}) \tag{10.21}$$

$$\mathcal{L}_{WW\gamma\gamma} = -e^2(W^-_\mu W^{+\mu} A_\nu A^\nu - W^-_\mu A^\mu W^+_\nu A^\nu) \tag{10.22}$$

$$\mathcal{L}_{WWZZ} = -g^2\cos^2\vartheta_{\rm w}(W^-_\mu W^{+\mu} Z_\nu Z^\nu - W^-_\mu Z^\mu W^+_\nu Z^\nu) \tag{10.23}$$

$$\mathcal{L}_{WWZ\gamma} = g^2\sin\vartheta_{\rm w}\cos\vartheta_{\rm w}(-2W^-_\mu W^{+\mu} A_\nu Z^\nu + W^-_\mu Z^\mu W^+_\nu A^\nu + W^-_\mu A^\mu W^+_\nu Z^\mu) \tag{10.24}$$

10.4 Higgs boson interactions

Let us start with the Higgs boson self-couplings; these are obtained readily from the potential part of $\mathcal{L}_{\rm Higgs}$ (see (10.6)) when substituting there the U-gauge form of the doublet ϕ ((10.9)). One has

$$\mathcal{L}_{\rm potential} = -\lambda\left(\frac{1}{2}(v+H)^2 - \frac{v^2}{2}\right)^2$$

There appear quartic and cubic self-interaction terms for the H, namely

$$\mathcal{L}_{HHH} = -\lambda v H^3 = -\frac{1}{4}g\frac{m_H^2}{m_W}H^3 \tag{10.25}$$

$$\mathcal{L}_{HHHH} = -\lambda\frac{1}{4}H^4 = -\frac{1}{32}g^2\frac{m_H^2}{m_W^2}H^4 \tag{10.26}$$

The interactions of the H with vector bosons and mass terms for the latter follow from the covariant derivatives in the $\mathcal{L}_{\rm Higgs}$. The relevant expression is

$$\mathcal{L} = \frac{1}{8}(v+H)^2\left(g^2\big((A^1_\mu)^2 + (A^2_\mu)^2\big) + g^2A^3_\mu A^{3\mu} - gg'A^3_\mu B^\mu + g'^2 B_\mu B^\mu\right)$$

Rewriting this in term of the $W^\pm$ and Z (see (10.10)), one gets

$$\mathcal{L} = \frac{1}{4}(v+H)^2 g^2 W^-_\mu W^{+\mu} + \frac{1}{8}(v+H)^2\frac{g}{\cos\vartheta_{\rm w}}Z_\mu Z^\mu \tag{10.27}$$

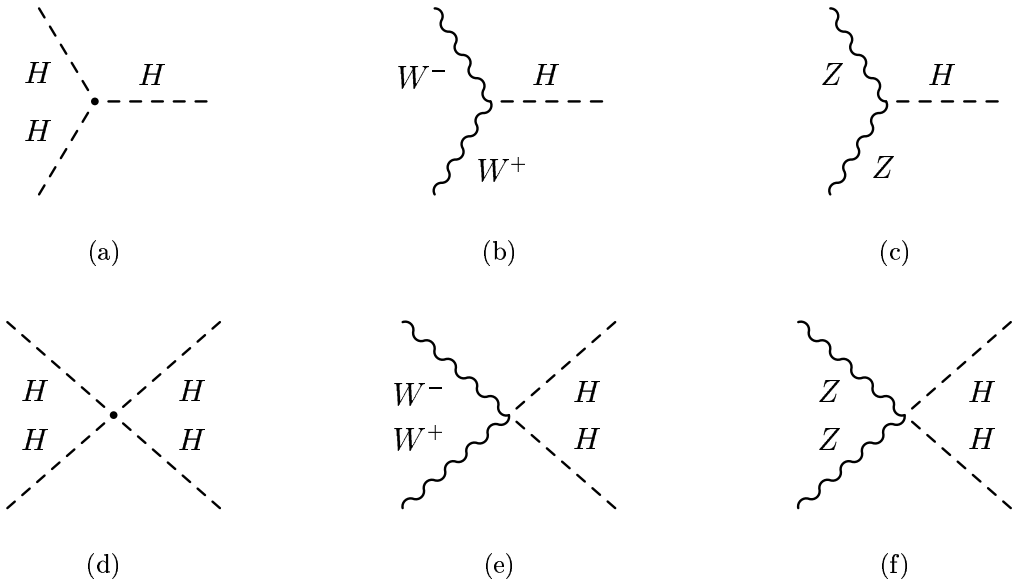

Figure 10.3: Higgs boson interactions

where one can identify these particular interactions:

$$\mathcal{L}_{WWH} = g m_W W^-_\mu W^{+\mu} H \tag{10.28}$$

$$\mathcal{L}_{WWZ} = \frac{g m_W}{2\cos^2\vartheta_{\rm W}} Z_\mu Z^\mu H \tag{10.29}$$

$$\mathcal{L}_{WWHH} = \frac{1}{4} g^2 W^-_\mu W^{+\mu} H H \tag{10.30}$$

$$\mathcal{L}_{ZZHH} = \frac{1}{8}(g^2 + g'^2) Z_\mu Z^\mu H H = \frac{g^2}{8\cos^2\vartheta_{\rm W}} Z_\mu Z^\mu H H \tag{10.31}$$

Note that the v^2 coming from the factor $(v+H)^2$ in (10.27) generates vector boson masses (10.11); therefore the coupling constants can be written as $(g_{VVH}/m_X^2) = 2/v$, $(g_{VVHH}/m_X^2) = v^{-2}$ (V is generic notation for vector boson), which after substitution $v = 2m_W/g$ yields the expressions shown above. It also makes it clear why there is no photon interaction with Higgs boson.

There are also interactions of the Higgs boson with fermions, obtained from (10.13)

$$\mathcal{L}_{\rm Yukawa} = -\frac{h_e}{\sqrt{2}}(v+H)(\bar{e}_L e_R + \bar{e}_R e_L)$$

which after using $\bar{e}_L e_R + \bar{e}_R e_L = \bar{e}e$ gives mass term with $m_e = v h_e/\sqrt{2}$ and consequently the Higgs-lepton interaction becomes

$$\mathcal{L}_{eeH} = -\frac{g}{2}\frac{m_e}{m_W}\bar{e}eH$$

The Higgs interaction with other fermions has the same form as the eeH interaction, after replacement $m_e \to m_f$, because they are due to the factor $(v+H)$.

Chapter 11

W and Z bosons – discovery and properties

(under construction:-)

Chapter 12

QCD and parton model summary

12.1 DIS and parton model

(under construction:-)

12.2 Some properties of parton distribution functions

I present here only some basic properties of parton distribution functions with emphasis on the straightforward physical interpretation, not concerning the scaling dependence nor their evolution.

- Naturally we require relations

$$f_q^p(x) = f_{\bar{q}}^{\bar{p}}(x)\,, \quad f_{\bar{q}}^p(x) = f_q^{\bar{p}}(x)\,,$$

  i.e. the probability density of "finding" a quark in proton should be the same as finding an antiquark in antiproton. Let us denote $f_u^p(x)$ simply as $u(x)$ and similarly for other quarks and gluons.

- integrals of the type

$$\int_0^1 q(x)\,\mathrm{d}x$$

  have obviously the meaning of the number of quarks of the given type in proton. However, they diverge suggesting their number to be infinite in some way.

- What makes sense is the momentum carried by a parton q (either quark or gluon) which is given by

$$P_q \equiv \int_0^1 x\,q(x)\,\mathrm{d}x\,.$$

- Experimental value for momentum carried by all quarks

$$\int_0^1 x\,[u(x) + \bar{u}(x) + d(x) + \bar{d}(x) + s(x) + \bar{s}(x) + c(x) + \bar{c}(x) + b(x) + \bar{b}(x)]\,\mathrm{d}x \doteq 0.5$$

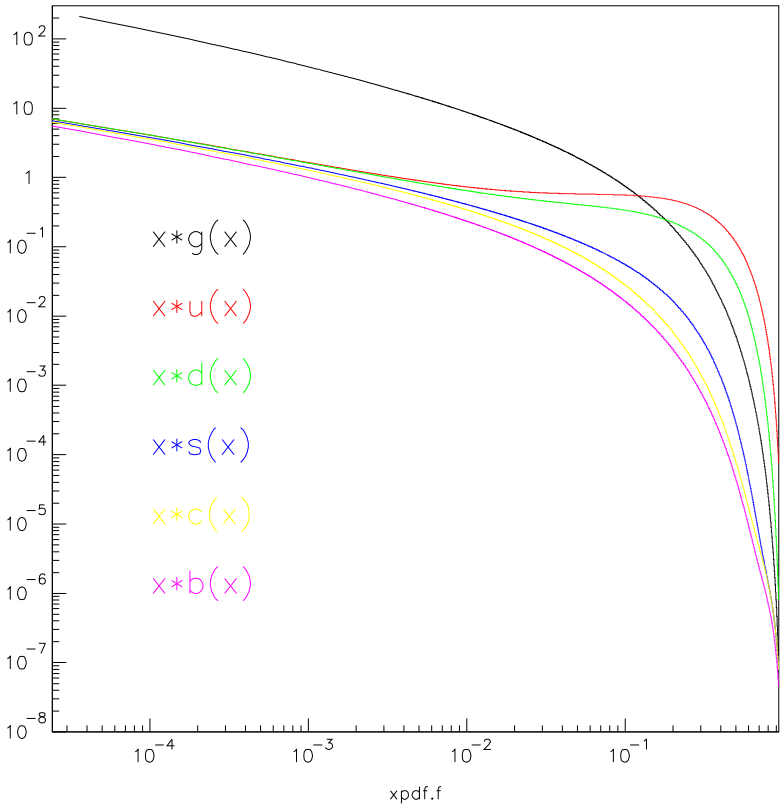

Figure 12.1: Functions $xq(x)$ plotted for $\mu_F = m_t$ for g, u, d, s, c, b.

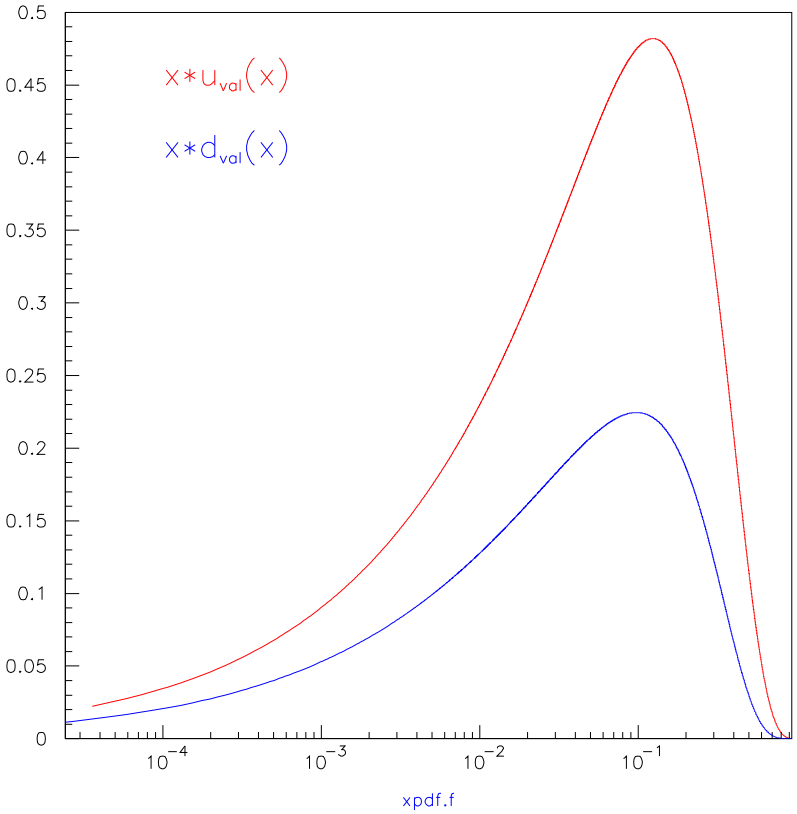

Figure 12.2: Functions $xu_{\mathrm{val}}(x)$ and $xd_{\mathrm{val}}(x)$ ploted for $\mu_F = m_t$.

suggests the there are neutral constituents – gluons – carrying about half of the proton's momentum!

- My values from numerical integrations over $x \in (10^{-6}, 1)$ using the CTEQ6 ([13]) set of PDF in LO for $\mu_F = m_t$ are

$$\begin{array}{lll} \mathbf{P_g = 0.478} & P_u = 0.211 & P_d = 0.112 \\ P_s = 0.0272 & P_{\bar{u}} = 0.0348 & P_{\bar{d}} = 0.0395 \\ P_c = 0.0206 & P_b = 0.0136 & \mathbf{P_{allq} = 0.520} \end{array}$$

- Defining valence and sea quark distributions as

$$\begin{gathered} u_{\mathrm{val}}(x) = u(x) - \bar{u}(x) \\ u_{\mathrm{sea}}(x) = \bar{u}(x)\,, \\ \text{so} \quad u(x) = u_{\mathrm{val}}(x) + u_{\mathrm{sea}}(x)\,, \\ \text{whereas} \quad s(x) = s_{\mathrm{sea}}(x)\,, \quad \bar{s}(x) = s_{\mathrm{sea}}(x) \quad s_{\mathrm{val}}(x) = 0 \end{gathered}$$

we may postulate the following relations as a conservation of proton's

$$\text{Charge}: \quad \int_0^1 \left\{ \frac{2}{3}[u_{\mathrm{val}}(x) + c_{\mathrm{val}}(x)] - \frac{1}{3}[d_{\mathrm{val}}(x) + s_{\mathrm{val}}(x) + b_{\mathrm{val}}(x)] \right\} \mathrm{d}x = 1\,,$$

$$\text{Baryon number}: \quad \int_0^1 \frac{1}{3}\left[u_{\mathrm{val}}(x) + d_{\mathrm{val}}(x) + s_{\mathrm{val}}(x) + c_{\mathrm{val}}(x) b_{\mathrm{val}}(x)\right] \mathrm{d}x = 1\,,$$

$$\text{Strangeness}: \quad \int_0^1 s_{\mathrm{val}}(x)\,\mathrm{d}x = 0\,,$$

$$\text{Charm}: \quad \int_0^1 c_{\mathrm{val}}(x)\,\mathrm{d}x = 0\,,$$

$$\text{Beauty}: \quad \int_0^1 b_{\mathrm{val}}(x)\,\mathrm{d}x = 0\,,$$

which imply

$$\int_0^1 u_{\mathrm{val}}(x)\,\mathrm{d}x = 2 \qquad \int_0^1 d_{\mathrm{val}}(x)\,\mathrm{d}x = 1\,.$$

These relations are important connection between the parton and the additive (constituent) quark model, where proton belongs to $SU(3)$ group octet with the "quark content" (uud). My results using the CTEQ6 ([13]) set of PDF in LO for $\mu_F = m_t$ are

$$\int_{10^{-6}}^1 u_{\mathrm{val}}(x)\,\mathrm{d}x \doteq 1.995 \qquad \int_{10^{-6}}^1 d_{\mathrm{val}}(x)\,\mathrm{d}x \doteq 0.998\,.$$

Actually, relations mentioned above are used as conditions for extracting PDFs from experimental data. However, once extracted, they are universal, i.e. regardless of a process we try to describe they provide us with a good agreement with experiment.

For further information see ([8]) and ([10]).

Part III

Examples and appendixes

Chapter 13

Some example calculations

13.1 Tree level decay width of the process $t \to W^+ + b$

According to the relevant part of the SM Lagrangian for this process

$$\mathcal{L} = \frac{g}{2\sqrt{2}} \left(\mathcal{J}_\rho W^{+\rho} + \mathcal{J}_\rho^\dagger W^{-\rho} \right) \tag{13.1}$$

$$\mathcal{J}_\rho \equiv V_{tb}\, \bar{b} \gamma_\rho (1 - \gamma_5) t$$

we may write the invariant amplitude

$$-i\mathcal{M}_{fi} = -i\frac{g}{2\sqrt{2}} V_{tb}\, \bar{u}(k) \gamma_\mu (1 - \gamma_5) u(P) \varepsilon^\mu(p, \lambda) \tag{13.2}$$

and squaring the absolute value of the expression (I do not explicitly write spin arguments of quarks)

$$|\mathcal{M}_{fi}|^2 = \frac{g^2}{8} |V_{tb}|^2 \bar{u}(k) \not{\varepsilon}(p, \lambda)(1 - \gamma_5) u(P) \bar{u}(P) \not{\varepsilon}^*(p, \lambda)(1 - \gamma_5) u(k)\,, \tag{13.3}$$

where V_{tb} is the element of the CKM matrix referring to the probability transition amplitude between these two quarks. Summing over final spins and averaging over the top quark spin we get

$$\overline{|\mathcal{M}_{fi}|^2} = \frac{g^2}{16} |V_{tb}|^2 \sum_{\lambda=-1}^{1} \varepsilon^\mu(p, \lambda) \varepsilon^{*\nu}(p, \lambda) \mathrm{Tr}[\gamma_\mu (1 - \gamma_5)(\not{P} + M) \gamma_\nu (1 - \gamma_5)(\not{k} + m)]\,. \tag{13.4}$$

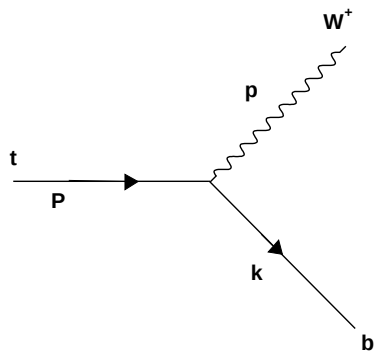

Figure 13.1: Tree level Feynman diagram for $t \to W^+ + b$.

Using identities

$$\sum_{\lambda=-1}^{1} \varepsilon^{\mu}(p,\lambda)\varepsilon^{*\nu}(p,\lambda) = -g^{\mu\nu} + \frac{1}{m_W^2} p^{\mu} p^{\nu} \tag{13.5}$$

$$\{\gamma_\mu, \gamma_5\} = 0 \quad \text{and} \quad \left[\frac{1}{2}(1 \pm \gamma_5)\right]^2 = \frac{1}{2}(1 \pm \gamma_5) \tag{13.6}$$

we find that the term proportional to $m_b m_t$ disappears due to anticommutation relations (and terms linear in masses due to the fact that trace of an odd number of gamma matrices is zero). Thus we have

$$\overline{|\mathcal{M}_{fi}|^2} = \frac{g^2}{8}|V_{tb}|^2 \left[-g^{\mu\nu} + \frac{1}{m_W^2} p^{\mu} p^{\nu}\right] \mathrm{Tr}[\not{P}\gamma_\nu \not{k}\gamma_\mu(1-\gamma_5)]\,, \tag{13.7}$$

of which the part containing γ_5 actually does not contribute after contracted with the symmetrical tensor in square brackets. Employing well known trace identities we arrive to an expression

$$\begin{aligned}\overline{|\mathcal{M}_{fi}|^2} &= \frac{g^2}{2}|V_{tb}|^2 \left[-g^{\mu\nu} + \frac{1}{m_W^2} p^{\mu} p^{\nu}\right] [P_\nu k_\mu - g_{\mu\nu}(P.k) + P_\mu k_\nu] \\ &= g^2|V_{tb}|^2 \left[\frac{1}{m_W^2}(p.k)(p.P) + (P.k) - \frac{1}{2m_W^2}(p.p)(P.k)\right]\,. \end{aligned} \tag{13.8}$$

Performing the evaluation of dot products in the rest system of the decaying top quark we find

$$P = (m_t, \vec{0}) \qquad k = (E_b^*, \vec{p}^{\,*}) \qquad p = (E_W^*, -\vec{p}^{\,*}) \tag{13.9}$$

$$E_b^* = \frac{m_t^2 + m_b^2 - m_W^2}{2m_t} \qquad E_W^* = \frac{m_t^2 - m_b^2 + m_W^2}{2m_t} \tag{13.10}$$

$$p^{*2} = \frac{[m_t^2 - (m_W - m_b)^2][m_t^2 - (m_W + m_b)^2]}{4m_t^2}\,. \tag{13.11}$$

Substituting these into

$$\overline{|\mathcal{M}_{fi}|^2} = \frac{g^2}{2}|V_{tb}|^2 \left[\frac{m_t E_W^*}{m_W^2}(E_b^* E_W^* + p^{*2}) + m_t E_b^* - \frac{m_t E_W^*}{2m_W^2}(E_W^{*2} - p^{*2})\right]$$

and after a half–page algebra we get the result (neglecting terms m_b^2/m_W^2)

$$\overline{|\mathcal{M}_{fi}|^2} = g^2|V_{tb}|^2 \frac{m_t^4}{4m_W^2}\left(1 - \frac{m_W^2}{m_t^2}\right)\left(1 + 2\frac{m_W^2}{m_t^2}\right)\,. \tag{13.12}$$

Recalling the expression for the decay width for the process $1 \to a + b$

$$\mathrm{d}\Gamma = \frac{1}{32\pi^2 s} p^* |\mathcal{M}_{fi}|^2 \mathrm{d}\Omega \tag{13.13}$$

and rewriting the coupling constant g it terms of m_W and Fermi coupling constant

$$\frac{G_\mathrm{F}}{\sqrt{2}} = \frac{g^2}{8m_W} \tag{13.14}$$

we finally obtain the decay width for $t \to W + b$

$$\Gamma_t = \frac{G_\mathrm{F} m_t^3}{8\pi\sqrt{2}}\left(1 - \frac{m_W^2}{m_t^2}\right)^2\left(1 + 2\frac{m_W^2}{m_t^2}\right) \tag{13.15}$$

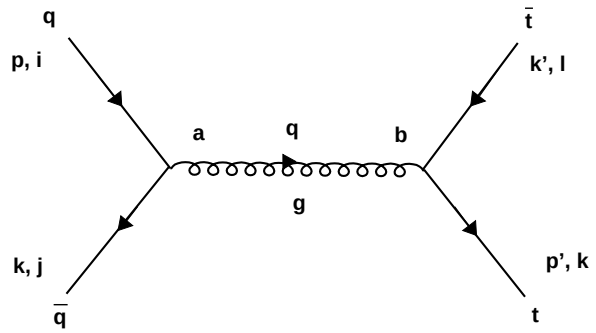

Figure 13.2: Leading Feynman diagram for the process $q\bar{q} \to t\bar{t}$.

Quark propagator:	$\delta^{ij}\dfrac{i}{(\not{p} - m + i\epsilon)}$
Gluon propagator:	$\delta^{ab}\dfrac{-ig_{\mu\nu}}{(p^2 + i\epsilon)}$
Interaction vertex:	$-ig(T^a)_{ij}\gamma_\mu$
Three gluon vertex:	$-gf^{abc}V^{\mu\nu\lambda}(p,q,r)$
	$= -gf^{abc}[g^{\mu\nu}(p-q)^\lambda + g^{\nu\lambda}(q-r)^\mu + g^{\lambda\mu}(r-p)^\nu]$

Table 13.1: QCD Feynman rules (Greek letters stand for Lorentz indices, Latin for colours).

13.2 $q\bar{q} \to t\bar{t}$ cross section

The relevant Feynman diagram is drawn in Figure 13.2. According to my notation the four-momentum conservation is $p + k = p' + k' = q$, $\quad q^2 = \hat{s}$. Using the following abbreviations for quark masses $m_q = m$ and $m_t = M$, the invariant amplitude for the process reads:

$$-i\mathcal{M}_{fi} = \frac{-i\delta^{ab}g^{\mu\nu}}{q^2}[\bar{v}_q^j(k)(-ig\gamma_\mu T^a_{ij})u_q^i(p)]\,[\bar{u}_t^k(p')(-ig\gamma_\nu T^b_{lk})v_t^l(k')] \tag{13.16}$$

$$\mathcal{M}_{fi} = \frac{g^2}{q^2}(T^a_{ij}T^a_{lk})[\bar{v}_q^j(k)\gamma^\mu u_q^i(p)][\bar{u}_t^k(p')\gamma_\mu v_t^l(k')]\,. \tag{13.17}$$

Summing over all final colours and averaging over initial ones we get

$$\frac{1}{9}\sum_{\text{colours}}\mathcal{M}_{fi}\mathcal{M}^*_{fi} = \frac{1}{9}\frac{g^4}{\hat{s}^2}(T^a_{ij}T^a_{lk}T^{b*}_{lk}T^{b*}_{ij})$$

$$\times\ \mathrm{Tr}[\gamma^\mu u_q(p)\bar{u}_q(p)\gamma^\nu v_q(k)\bar{v}_q(k)]\ \mathrm{Tr}[\gamma_\mu v_t(k')\bar{v}_t(k')\gamma_\nu u_t(p')\bar{u}_t(p')] \tag{13.18}$$

and reordering the elements of $SU(3)$ matrices we get

$$\sum_{a,b,i,j,k,l} T^a_{ij}T^{*b}_{ji}T^a_{lk}T^{b*}_{kl} = \sum_{a,b}\mathrm{Tr}(T^aT^{b\dagger})\mathrm{Tr}(T^aT^{b\dagger}) = \sum_{a,b}\mathrm{Tr}(T^aT^b)\mathrm{Tr}(T^aT^b) \tag{13.19}$$

$$= \sum_{a,b} \frac{1}{4}\delta^{ab}\delta^{ab} = \frac{1}{4}\mathrm{Tr}(\delta^2) = \frac{8}{4} = 2\,.$$

where we used the colour trace identity

$$\mathrm{Tr}(T^a T^b) = \frac{1}{2}\delta^{ab}\,. \tag{13.20}$$

Now summing and averaging over spins we obtain

$$\overline{|\mathcal{M}_{fi}|^2} \equiv \frac{1}{9}\frac{1}{4}\sum_{\substack{\text{spins}\\ \text{colours}}} |\mathcal{M}_{fi}|^2 = \frac{g^4}{18\hat{s}^2}\,\mathrm{Tr}[\gamma^\mu(\not{p}+m)\gamma^\nu(\not{k}-m)]\,\mathrm{Tr}[\gamma_\mu(\not{k}'-M)\gamma_\nu(\not{p}'+M)]\,. \tag{13.21}$$

Neglecting the initial quark masses m, the only surviving traces are

$$\mathrm{Tr}(\gamma^\mu\not{p}\gamma^\nu\not{k})\,[\mathrm{Tr}(\gamma_\mu\not{k}'\gamma_\nu\not{p}') - M^2\mathrm{Tr}(\gamma_\mu\gamma_\nu)] = 32[(p.k')(k.p') + (p.p')(k.k') + M^2(p.k)] \tag{13.22}$$

Working out dot products from Mandelstam variables

$$\begin{aligned} \hat{s} &\equiv (p+k)^2 = (p'+k')^2 \\ \hat{t} &\equiv (p-p')^2 = (k-k')^2 \\ \hat{u} &\equiv (p-k')^2 = (p'-k)^2 \end{aligned} \tag{13.23}$$

$$(p.k') = (p'.k) = \frac{M^2-\hat{u}}{2} \qquad (k.k') = (p.p') = \frac{M^2-\hat{t}}{2} \tag{13.24}$$

$$(p.k) = \frac{\hat{s}}{2} \qquad (p'.k') = \frac{\hat{s}}{2} - M^2 \tag{13.25}$$

and introducing α_s as $g^2 = 4\pi\alpha_s$ we arrive at

$$\overline{|\mathcal{M}_{fi}|^2} = \frac{64\pi^2}{9}\alpha_s^2\frac{[(\hat{u}-M^2)^2 + (\hat{t}-M^2)^2 + 2\hat{s}M^2]}{\hat{s}^2}\,. \tag{13.26}$$

Using the expression for the cross section in CMS frame

$$\frac{\mathrm{d}\sigma}{\mathrm{d}\Omega^*} = \frac{1}{64\pi^2\hat{s}}\frac{|\vec{p}_f^{\,*}|}{|\vec{p}_i^{\,*}|}|\mathcal{M}_{fi}|^2\,, \tag{13.27}$$

where in our case

$$|\vec{p}_f^{\,*}| = \frac{\sqrt{\hat{s}-4M^2}}{2} \tag{13.28}$$

$$|\vec{p}_i^{\,*}| = \frac{\sqrt{\hat{s}}}{2} \tag{13.29}$$

$$\hat{t} = M^2 - \frac{\hat{s}}{2}\left(1 - \sqrt{1-\frac{4M^2}{\hat{s}}}\cos\theta^*\right) \tag{13.30}$$

$$\hat{u} = M^2 - \frac{\hat{s}}{2}\left(1 + \sqrt{1-\frac{4M^2}{\hat{s}}}\cos\theta^*\right) \tag{13.31}$$

we find the expression for the differential cross section

$$\frac{\mathrm{d}\hat{\sigma}_{q\bar{q}\to t\bar{t}}}{\mathrm{d}\cos\theta^*} = \frac{\pi\alpha_s^2}{9\hat{s}^2}\sqrt{1-\frac{4M^2}{\hat{s}}}\left[(\hat{s}+4M^2)+(\hat{s}-4M^2)\cos^2\theta^*\right]. \tag{13.32}$$

We see that the angular dependence vanishes as we are approaching the threshold for the $t\bar{t}$ production. Finally after integration over the angle the cross section yields

$$\hat{\sigma}_{q\bar{q}\to t\bar{t}}(\hat{s}) = \frac{8\pi}{27}\frac{\alpha_s^2}{\hat{s}^2}\sqrt{1-\frac{4M^2}{\hat{s}}}\,(\hat{s}+2M^2). \tag{13.33}$$

13.3 $gg \to t\bar{t}$ cross section

This section should serve only as an illustration of what can cross sections look like and behave, one should notice the angular dependence of different channels reflecting the structures in propagators.

Having three diagrams in game, we have the diagonal $\hat{s}$, $\hat{t}$, $\hat{u}$ channels contributions

$$\overline{|\mathcal{M}_{fi}^{ss}|^2} = 12\pi^2\alpha_s^2\frac{(M^2-\hat{t})(M^2-\hat{u})}{\hat{s}^2} \tag{13.34}$$

$$\overline{|\mathcal{M}_{fi}^{tt}|^2} = \frac{8}{3}\pi^2\alpha_s^2\frac{(M^2-\hat{t})(M^2-\hat{u})-2M^2(M^2+\hat{t})}{(M^2-\hat{t})^2} \tag{13.35}$$

$$\overline{|\mathcal{M}_{fi}^{uu}|^2} = \frac{8}{3}\pi^2\alpha_s^2\frac{(M^2-\hat{t})(M^2-\hat{u})-2M^2(M^2+\hat{u})}{(M^2-\hat{u})^2} \tag{13.36}$$

as well as three negative interference terms

$$\overline{|\mathcal{M}_{fi}^{tu}|^2} = -\frac{2}{3}\pi^2\alpha_s^2\frac{2M^2(\hat{s}-4M^2)}{(M^2-\hat{u})(M^2-\hat{t})} \tag{13.37}$$

$$\overline{|\mathcal{M}_{fi}^{st}|^2} = -6\pi^2\alpha_s^2\frac{(M^2-\hat{t})(M^2-\hat{u})+M^2(\hat{u}-\hat{t})}{\hat{s}(M^2-\hat{t})} \tag{13.38}$$

$$\overline{|\mathcal{M}_{fi}^{su}|^2} = -6\pi^2\alpha_s^2\frac{(M^2-\hat{t})(M^2-\hat{u})+M^2(\hat{t}-\hat{u})}{\hat{s}(M^2-\hat{u})}. \tag{13.39}$$

The result of the integration over $\hat{t}$ with

$$t_{max} = M^2 - \frac{\hat{s}}{2}\left(1-\sqrt{1-\frac{4M^2}{\hat{s}}}\right)$$

$$t_{min} = M^2 - \frac{\hat{s}}{2}\left(1+\sqrt{1-\frac{4M^2}{\hat{s}}}\right)$$

is (taken from Combridge, 1979)

$$\hat{\sigma}_{gg\to t\bar{t}}(\hat{s}) = \frac{\pi}{3}\frac{\alpha_s^2}{\hat{s}}\left[-\left(7+\frac{31M^2}{\hat{s}}\right)\frac{1}{4}\chi+\left(1+\frac{4M^2}{\hat{s}}+\frac{M^4}{\hat{s}^2}\right)\ln\frac{1+\chi}{1-\chi}\right] \tag{13.40}$$

with

$$\chi \equiv \sqrt{1-\frac{4M^2}{\hat{s}}}.$$

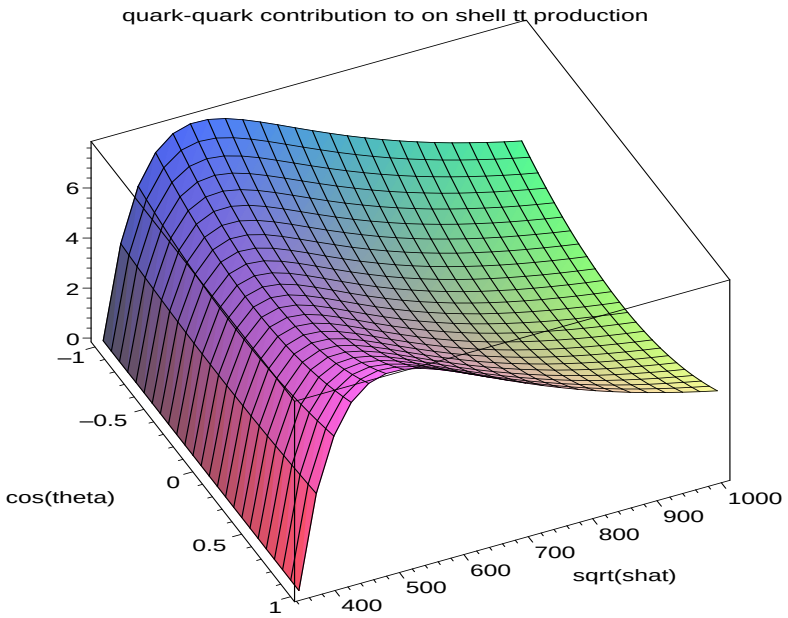

Figure 13.3: Differential cross section $\hat{\sigma}_{q\bar{q}\to t\bar{t}}$ in pb as a function of $\cos\theta^*$ and $\sqrt{\hat{s}}$ in GeV.

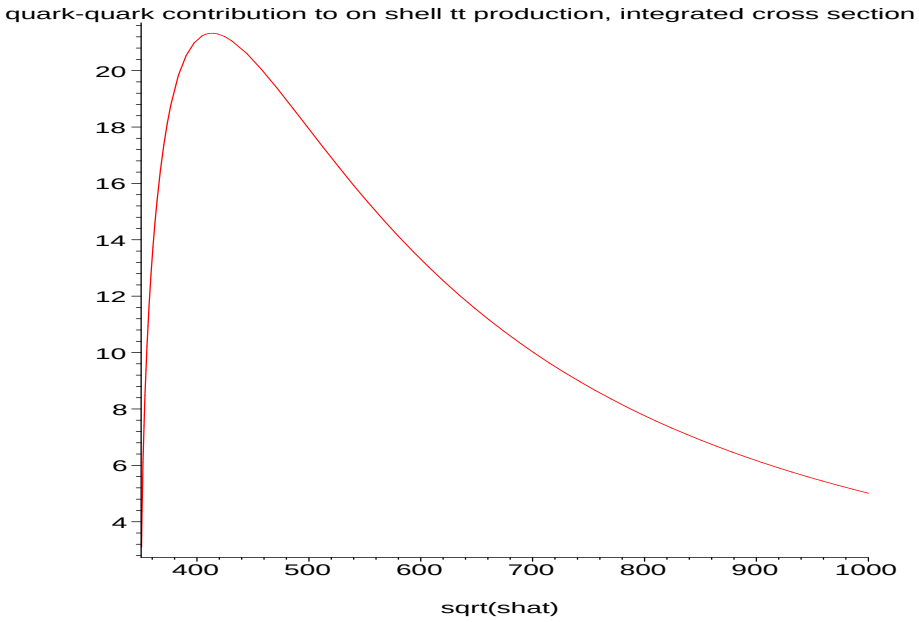

Figure 13.4: Integrated cross section $\hat{\sigma}_{q\bar{q}\to t\bar{t}}$ in pb as a function of $\sqrt{\hat{s}}$ in GeV.

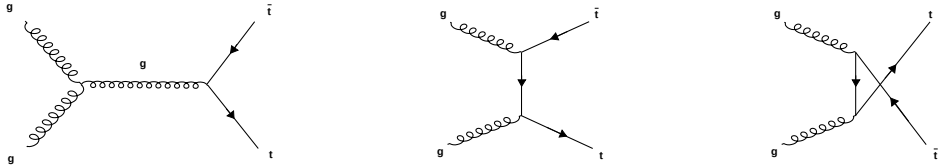

Figure 13.5: Feynman diagrams for the process $gg \to t\bar{t}$.

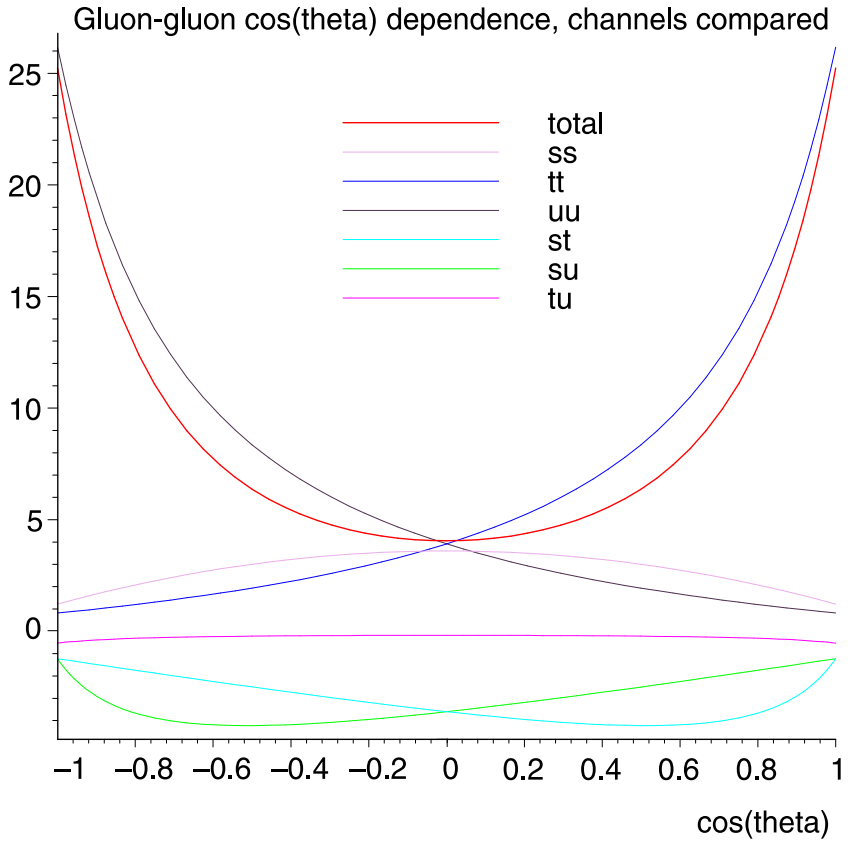

Figure 13.6: Differential cross section $\hat{\sigma}_{gg\to t\bar{t}}$ in pb as a function of $\cos\theta^*$ for $\sqrt{\hat{s}} = 600\,\text{GeV}$.

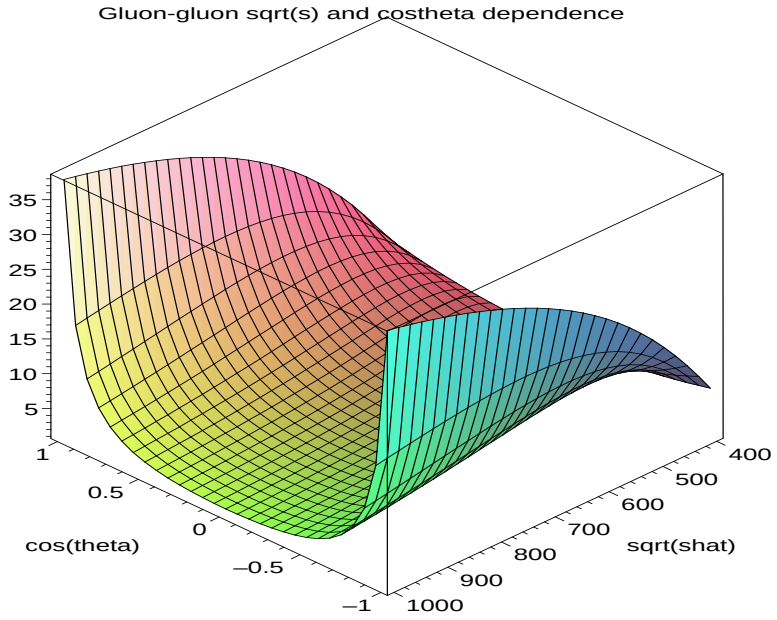

Figure 13.7: Differential cross section $\hat{\sigma}_{gg\to t\bar{t}}$ in pb as a function of $\cos\theta^*$ and $\sqrt{\hat{s}}$ in GeV.

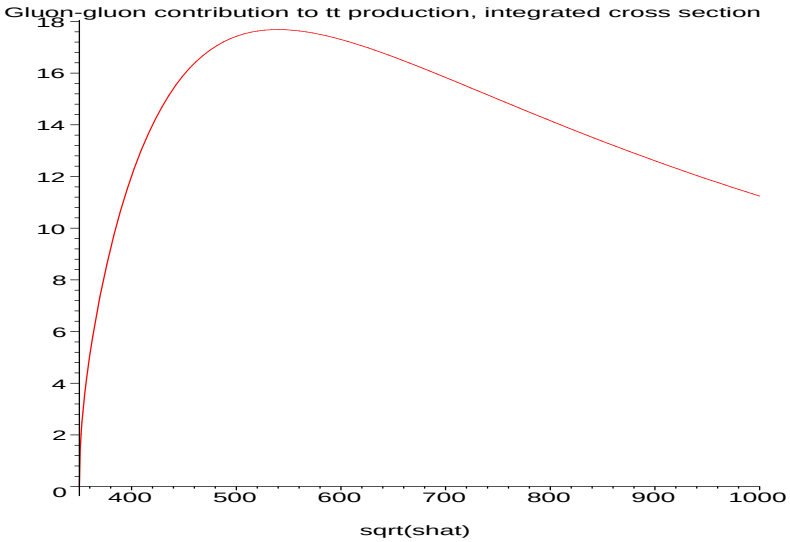

Figure 13.8: Integrated cross section $\hat{\sigma}_{gg\to t\bar{t}}$ in pb as a function of $\sqrt{\hat{s}}$ in GeV.

Chapter 14

Useful relations

14.1 Relativistic kinematics

$$\beta = \text{velocity} \qquad m = \text{rest mass} \qquad \gamma = \frac{1}{\sqrt{1-\beta^2}}$$

$$E = \sqrt{\vec{p}^{\,2} + m^2} \qquad E = T + m \qquad T = (\gamma - 1)\, m$$

$$E = \gamma m \qquad \vec{p} = \vec{\beta}\gamma m \qquad \vec{\beta} = \frac{\vec{p}}{E}$$

Table 14.1: Basic kinematics formulæ

14.2 Transformation properties of rapidity

The rapidity of a particle with respect to the z axis is defined as

$$y = \frac{1}{2} \ln \left(\frac{E + p_z}{E - p_z} \right) . \tag{14.1}$$

Let us suppose a boost along the z axis so that

$$E' = \gamma(E - \beta p_z)$$

$$p'_z = \gamma(p_z - \beta E) .$$

Then the transformed rapidity is

$$y' = \frac{1}{2} \ln \left(\frac{E - \beta p_z + p_z - \beta E}{E - \beta p_z - p_z + \beta E} \right) = \frac{1}{2} \ln \left(\frac{E + p_z}{E - p_z} \frac{1 - \beta}{1 + \beta} \right) . \tag{14.2}$$

Inverting the hyperbolic tangent

$$\tanh = \frac{e^y - e^{-y}}{e^y + e^{-y}} = \frac{e^{2y} - 1}{e^{2y} + 1}$$

we get

$$\text{arctanh } x = \ln \sqrt{\frac{1+x}{1-x}}\,, \tag{14.3}$$

so we see that

$$y' = y + \ln \sqrt{\frac{1-\beta}{1+\beta}} = y - \text{arctanh } \beta\,. \tag{14.4}$$

Thus when given the number of events as a function of rapidity, the rapidity distribution remains unchanged

$$\frac{\mathrm{d}N(y)}{\mathrm{d}y} = \frac{\mathrm{d}N'(y')}{\mathrm{d}y'}\,.$$

Another often used quantity is the pseudorapidity

$$\eta = -\ln \tan \frac{\theta}{2}\,. \tag{14.5}$$

Following limit holds: $y \to \eta$ for $m \ll E$ and $\theta \gg \frac{1}{\gamma}$.

14.3 Some useful relations for QFT calculations

- Conventions for scattering and invariant amplitudes:

$$S_{fi} \equiv \delta_{fi} - i(2\pi)^4 \delta^{(4)}\,(P_f - P_i)\,T_{fi}$$

$$S_{fi} \equiv \langle f|\hat{S}|i\rangle \qquad \langle f|i\rangle \equiv \delta_{fi}$$

$$\mathcal{M}_{fi} \equiv T_{fi} \prod_{j=1}^{n_f+n_i} (2\pi)^{3/2}\sqrt{2E_j}$$

$$\text{dimensionality}: \quad [\mathcal{M}_{fi}] = M^{4-n}, \qquad n = n_f + n_i$$

  with the fields normalisations (here for example in case of a charged fermion)

$$\hat{\psi}(x) = \frac{1}{(2\pi)^{3/2}} \int \frac{\mathrm{d}^3 p}{\sqrt{2E(p)}} \sum_{s=1}^{2} \left[\hat{a}(p,s)u(p,s)e^{-ip\cdot x} + \hat{a}^\dagger(p,s)v(p,s)e^{ip\cdot x}\right]$$

  Lorentz invariant phase space:

$$\mathrm{dLips}_n(s, p_1, \ldots, p_n) \equiv (2\pi)^4 \delta^{(4)}(P_f - P_i) \prod_{j=1}^{n} \frac{\mathrm{d}^3 \vec{p}_j}{(2\pi)^3 2E_j}$$

$$\text{Two body phase space: } \frac{1}{4\pi}\frac{p^*}{\sqrt{s}}$$

- Dirac equation, positive and negative plain wave solutions:

$$(i\gamma^\mu \partial_\mu - m)\psi(x) = 0$$

$$\{\gamma^\mu, \gamma^\nu\} = 2g^{\mu\nu} \qquad \bar{u}(p) \equiv u^\dagger(p)\gamma_0$$

$$\gamma_0\gamma_\mu^\dagger\gamma_0 = \gamma_\mu \qquad g^{\mu\nu} = \mathrm{diag}(1,-1,-1,-1,-1)$$

In the standard realisation of the Clifford algebra

$$\gamma_0 = \begin{pmatrix} 1 & 0 \\ 0 & -1 \end{pmatrix} \qquad \vec{\gamma} = \begin{pmatrix} 0 & \vec{\sigma} \\ -\vec{\sigma} & 0 \end{pmatrix}$$

$$\begin{aligned} \psi_+ = u(p)e^{-ip.x} \qquad & \psi_- = v(p)e^{ip.x} \\ (\not{p} - m)u(p) = 0 \qquad & (\not{p} + m)v(p) = 0 \\ \bar{u}(p)u(p) = 2m \qquad & \bar{v}(p)v(p) = -2m \end{aligned}$$

$$\begin{aligned} u^{(s)}(p) &= \sqrt{E+m}\begin{pmatrix} \chi^{(s)} \\ \frac{\vec{\sigma}.\vec{p}}{E+m}\chi^{(s)} \end{pmatrix} \\ v^{(s)}(p) &= -\sqrt{E+m}\begin{pmatrix} \frac{\vec{\sigma}.\vec{p}}{E+m}\chi^{(s)} \\ \chi^{(s)} \end{pmatrix} \end{aligned}$$

- Projectors on energy and spin eigenstates ($\gamma_5 \equiv i\gamma_0\gamma_1\gamma_2\gamma_3$, $\{\gamma_5, \gamma_\mu\}=0$)

Spin fourvector satisfies : $\quad (s.p) = 0 \quad s^2 = -1$

$$\begin{aligned} u(p,s)\bar{u}(p,s) &= \frac{1}{2}(\not{p} + m)(1 + \gamma_5\not{s}) \\ v(p,s)\bar{v}(p,s) &= \frac{1}{2}(\not{p} - m)(1 + \gamma_5\not{s}) \\ \sum_{\pm s} u(p,s)\bar{u}(p,s) &= (\not{p} + m) \\ \sum_{\pm s} v(p,s)\bar{v}(p,s) &= (\not{p} - m) \end{aligned}$$

- Projectors on energy and helicity eigenstates ($\lambda = \pm\frac{1}{2}$)

$$\begin{aligned} u(p,\lambda)\bar{u}(p,\lambda) &= \frac{1}{2}(\not{p} + m)(1 + 2\lambda\gamma_5) \\ v(p,\lambda)\bar{v}(p,\lambda) &= \frac{1}{2}(\not{p} - m)(1 + 2\lambda\gamma_5) \end{aligned}$$

Spin fourvectors for describing helicity states, $m \neq 0$

$$s_R(k) = \left(\frac{|\vec{k}|}{m}, \frac{E}{m}\frac{\vec{k}}{|\vec{k}|}\right) \qquad s_L(k) \equiv -s_R(k)$$

- Chiral components:

$$\begin{aligned} u_R \equiv \frac{1}{2}(1+\gamma_5)\,u \qquad & u_L \equiv \frac{1}{2}(1-\gamma_5)\,u \\ v_R \equiv \frac{1}{2}(1-\gamma_5)\,v \qquad & v_L \equiv \frac{1}{2}(1+\gamma_5)\,v \\ u_L\bar{u}_L = \frac{1}{2}\not{p}\,(1+\gamma_5) \qquad & v_L\bar{v}_L = \frac{1}{2}\not{p}\,(1-\gamma_5) \\ u_R\bar{u}_R = \frac{1}{2}\not{p}\,(1-\gamma_5) \qquad & v_R\bar{v}_R = \frac{1}{2}\not{p}\,(1+\gamma_5) \end{aligned}$$

- Trace theorems (the Feynman symbol: $\not{a} \equiv a_\mu \gamma^u$)

$$\begin{aligned}
\mathrm{Tr}(\not{a}\not{b}) &= 4\,(a.b) \\
\mathrm{Tr}(\not{a}\not{b}\not{c}\not{d}) &= 4\ \ [(a.b)(c.d) - (a.c)(b.d) + (a.d)(b.c)] \\
\mathrm{Tr}(\not{a}\gamma_\rho\not{b}\gamma_\sigma)\mathrm{Tr}(\not{c}\gamma^\rho\not{d}\gamma^\sigma) &= 32\,[(a.c)(b.d) + (a.d)(b.c)] \\
\mathrm{Tr}(\not{a}\gamma_\rho\not{b}\gamma_\sigma\gamma_5)\mathrm{Tr}(\not{c}\gamma^\rho\not{d}\gamma^\sigma\gamma_5) &= 32\,[(a.c)(b.d) - (a.d)(b.c)] \\
\mathrm{Tr}(\not{a}\gamma_\rho\not{b}\gamma_\sigma\gamma_5)\mathrm{Tr}(\not{c}\gamma^\rho\not{d}\gamma^\sigma) &= 0 \\
\mathrm{Tr}(\gamma_\mu\gamma_\nu\gamma_\rho\gamma_\sigma\gamma_5) &= 4i\varepsilon_{\mu\nu\rho\sigma} \qquad \text{with} \quad \varepsilon_{0123} = 1
\end{aligned}$$

- Relations for reducing the number of γ matrices:

$$\begin{aligned}
\gamma_\mu\gamma^\mu &= 4 \\
\gamma_\mu\not{a}\gamma^\mu &= -2\not{a} \\
\gamma_\mu\not{a}\not{b}\gamma^\mu &= 4(a.b) \\
\gamma_\mu\not{a}\not{b}\not{c}\gamma^\mu &= -2\not{c}\not{b}\not{a} \\
\gamma_\mu\not{a}\not{b}\not{c}\not{d}\gamma^\mu &= 2(\not{b}\not{c}\not{d}\not{a} - \not{a}\not{d}\not{c}\not{b})
\end{aligned}$$

Chapter 15

Some historical milestones

15.1 Historical overview

Brief historical overview: (taken from Ronald Poling's syllabus to "Intro to Nuclear and Particle Physics", http://www.physics.umn.edu/classes/s4511/Chronology.pdf)

1873 Maxwell's theory of E&M.

1895 Röntgen's discovery of X-rays.

1898 The Curies separate radioactive elements.Thomson measures electron e/m: proposes "plum pudding" atom.

1900 Planck explains blackbody radiation with quantisation, but doesn't believe it.

1905 Einstein explains photoelectric effect with light quantum and believes it (dual particle-wave nature of photon).Einstein comes to grips with Maxwell, asserts that light speed is c for all observers and follows this to inevitable consequences: equivalence of mass and energy, special relativity.

1911 Rutherford interprets experiments of Geiger and Marsden. Alpha particles scattered at large angles from gold show atom has small, dense, positively charged nucleus.

1913 Bohr constructs a theory of atomic structure based on quantum ideas.

1919 Rutherford presents evidence of proton: heavier nuclei composed of hydrogen nuclei.

1921 Chadwick and Bieler suggest "strong force" holding the nucleus together.

1923 Compton confirms particle nature of photon (X-ray).

1920's Quantum mechanics developed by Bohr, Schrödinger, de Broglie, Pauli, Born, Heisenberg, and (combining quantum mechanics and special relativity) Dirac.

1927 Discovery of beta–decay, with continuous energy spectrum that led to...

1930 Pauli's suggestion of neutrino carrying off the rest of the energy in beta–decay.

1931 Chadwick discovers neutron, launching intensive study of nuclear binding and decay.

1933 Anderson discovers the positron, recognised as positively-charged counterpart to the electron. This is the first demonstration of antimatter, predicted by Dirac.

1934 Fermi presents theory of beta decay, introducing the weak interaction.

1935 Yukawa describes nuclear interactions by exchange of particles "mesons") between protons and neutrons. From nuclear size, Yukawa concludes mass of mesons ≈200 electron masses.

1937 Muon discovered in cosmic rays, mistakenly identified as Yukawa's meson.

1947 Muon recognised as incompatible with being Yukawa's meson, classified as a lepton, a heavier copy of the electron. Rabi complains "Who ordered that?"

1947 Pion (meson) discovered in cosmic rays, based on strong interactions in matter declared to be the true Yukawa meson.

1947 ... Feynman, Schwinger, Tomonaga, and others develop quantum electrodynamics: procedures to calculate electromagnetic interactions, properties of electrons, positrons, and photons. Tools include Feynman diagrams.

1948 The Berkeley synchro-cyclotron produces the first artificial pions, followed by neutral pion discovery in 1950.

1949 K^+ meson discovered, begins parade of "strange" particles: "V" particles (Λ^0 and K^0) in 1951, "delta" particles (Δ^{++}, Δ^+, Δ^0, and Δ^-) in 1952.

1952 Glaser invents bubble chamber, Brookhaven Cosmotron (1.3 GeV protons), starts operation, begins population explosion of "particle zoo."

1953–57 Scattering of electrons on nuclei measures charge density distribution inside protons and neutrons, with hints of internal structure.

1954 Yang and Mills formulate general framework of "gauge theories," basic element of Standard Model.

1955 Berkeley Bevatron starts operation; Chamberlain and Segre discover antiproton.

1956 Lee and Yang speculate that weak interaction might violate parity conservation (mirror symmetry) and C.S. Wu quickly demonstrates it in Cobalt–60 beta decays.

1957 Schwinger, Glashow, others lay foundations for unification of electromagnetic and weak interactions, including (although not naming) the weak intermediate vector bosons W^+ and W^-.

1961-64 Gell-Mann, Ne'eman, Zweig postulate quarks (u, d, s) to explain the zoo of particles and their regular patterns. (Think Mendeleev.)

1962 Lederman, Schwartz, Steinberger verify two distinct types of neutrinos (electron and muon neutrinos).

1964 Glashow, Bjorken speculate about existence of a fourth quark, dubbing it charm (c).

1965 Cronin and Fitch observe CP violation in K-meson decays.

1965 Greenberg, Han, Nambu introduce the quark property of colour charge. This becomes the basis for development in early '70's of strong interaction theory, QCD, showing "asymptotic freedom (Politzer, Gross, Wilczek).

1967 Weinberg, Salam independently propose unification of electromagnetic and weak interactions (electroweak). Theory predicts existence of a neutral vector boson Z^0.

1969 Bjorken and Feynman interpret "deep inelastic scattering" data (electrons on nuclei at SLAC) as demonstrating point-like constituents of the proton. Cautious interpretation: "partons," not yet demonstrated to be the hypothetical quarks.

1973 Observation of "neutral currents": weak interactions with no charge exchanged, indicating mediation by Z^0.

1974 J/ψ particle composed of charm and anti-charm quarks observed independently by Richter at SLAC and Ting at Brookhaven.

1976 Goldhaber and Pierre find the D^0-meson (anti-up and charm quarks) at SLAC.

1976 The tau lepton is discovered by Perl and collaborators at SLAC.

1978 Lederman and collaborators at Fermilab discover the b-quark.

1979 Evidence for gluon (strong interaction mediator) emission at DESY.

1983 Discovery of $W^{\pm}$ and Z^0 at CERN by group led by Rubbia.

1989 Measurement of Z^0 width at LEP (CERN) demonstrates exactly three generations of quarks and leptons.

1995 Discovery of the top quark at Fermilab by the CDF and DØ experiments.

1998 Observation of neutrino oscillations (i.e. nonzero neutrino mass) by Super-K collaboration.

2000 Observation of the tau neutrino by Lundberg, Fermilab

2000–1 Observation of CP violation using B-mesons by BABAR, BELLE experiments.

15.2 On the latest discovered elementary particle

Perhaps surprisingly for someone, this is not the famous top quark, but ...(Physics News Update, The American Institute of Physics Bulletin of Physics News Number 495 (Story #1), July 20, 2000 by Phillip F. Schewe and Ben Stein,
http://www.aip.org/enews/physnews/2000/split/pnu495-1.htm)

> ..."the evidence for the tau neutrino is slim but impressive: five scattering events are being exhibited at the seminar by Fermilab physicist Byron Lundberg, leader of Experiment 872, the Direct Observation of Nu Tau (or DONUT) collaboration (http://fn872.fnal.gov/). Their experiment proceeds in the following manner. Fermilab's 900-GeV proton beam (the highest beam energy in the world) was steered onto a tungsten target, where some of the prodigious incoming energy is

turned into new particles. Some of these quickly decay into taus and tau neutrinos. Next comes an obstacle course of magnets (meant to deflect charged particles away) and shielding material (meant to absorb most of the other particles except for rarely interacting neutrinos). Beyond this lies a sequence of emulsion targets in which the neutrinos can interact, leaving a characteristic signature.

Evidence for a tau neutrino in the emulsion is the creation of a tau lepton, which itself quickly decays (after travelling about 1 mm) into other particles. The E872 physicists estimate that about 1014 tau neutrinos entered the emulsion, of which perhaps 100 interacted therein. It is a carefully analysed handful of such events that is now being presented to the public in evidence. The tau neutrino is the third neutrino type to be detected. The detection of the electron neutrino by Clyde Cowan and Frederick Reines garnered Reines the 1995 Nobel Prize for physics (Cowan had died some years before). For discovering the muon neutrino, Leon Lederman, Melvin Schwartz, and Jack Steinberger won the Nobel Prize in 1988."

Bibliography

[1] J. D. Bjorken – S. D. Drell, *Relativistic Quantum Mechanics* and *Relativistic Quantum Fields*, McGraw–Hill, New York 1964 and 1965

[2] Vernon D. Barger–Roger J. N. Phillips, *Collider Physics*, Addison–Wesley, 1987

[3] I. J. R. Aitchinson – A. J. G. Hey, *Gauge Theories in Particle Physics*, Adam Hilger Bristol and Philadelphia 1989, second edition

[4] M. Riordan, *The Hunting of the Quark*, Simon& Schuster 1987

[5] Jiří Formánek, *Úvod do kvantové teorie*, Academia, Praha, 1983

[6] Jiří Formánek, *Úvod do kvantové teorie pole 1, 2a, 2b*, Karolinum, Praha, 2000

[7] Jiří Hořejší, *Fundamentals of Electroweak Theory*, Karolinum, Praha 2002
available at www–hep2.fzu.cz/Centrum

[8] Jiří Chýla, *Quarks, Partons and Quantum Chromodynamics*,
available at www–hep2.fzu.cz/Centrum, 2003

[9] Miro Kladiva, *Estimates of Higgs particle masses*, 2003, Diploma thesis, Charles University, Prague

[10] Karel Kolář, *QCD Evolution Equations and Their Solution*, 2003, Diploma thesis, Charles University, Prague

[11] *Particle Data Group*, http://pdg.lbl.gov

[12] *CernLib*, CERN Program Library, http://cernlib.web.cern.ch/cernlib/

[13] *CTEQ collaboration*, The Coordinated Theoretical–Experimental Project on QCD, CTEQ6 set of parton distribution functions, http://www.phys.psu.edu/~cteq/

[14] *PAW – Physics Analysis Workstation*, http://paw.web.cern.ch/paw/

[15] *ROOT – An Object–Oriented Data Analysis Framework*, http://root.cern.ch/

[16] W. Venus: *A LEP summary*, plenary talk at Europhysics Conference on High Energy Physics, Budapest 2001, published in the JHEP Proceedings, hep2001/284

[17] S. L. Glashow, Nucl. Phys. **22** (1961) 579.

S. Weinberg, Phys. Rev. Lett. **19** (1967) 1264.

A. Salam: *in Elementary Particle Physics*, Proc. Nobel Symposium No.**8** (ed. N. Svartholm, Almqvist & Wiksell, Sockholm 1968),p. 367

[18] G. 't Hooft and M. J. Veltman, Nucl. Phys. B **44** (1972) 189.
G. 't Hooft, Nucl. Phys. B **35** (1971) 167.